ANALYSIS AND MODELING OF NANO PHYSICS BASED DEVICES: (CNTFETs)

DISSERTATION

SUBMITTED IN PARTIAL FULFILMENT OF THE REQUIREMENTS
FOR THE AWARD OF THE DEGREE OF

Master of Philosophy

IN

Applied Physics

BY

PARVEJ AHMAD ALVI

Under the supervision of

Prof. K.M. Lal

Deptt. of Applied Physics

Under the co-supervision of

Dr. M.J. Siddiqui

Deptt. of Electronics Engg.

DEPARTMENT OF APPLIED PHYSICS
Z.H. COLLEGE OF ENGINEERING AND TECHNOLOGY
ALIGARH MUSLIM UNIVERSITY
ALIGARH (INDIA)

2004

Dedicated

to my

Lord (Allah)

Dr. K. M. Lal
(Professor & Chairman)

DEPARTMENT OF APPLIED PHYSICS
Z. H. COLLEGE OF ENGG. & TECH.
ALIGARH MUSLIM UNIVERSITY
ALIGARH-202 002, INDIA
Phone : Off. (0571) 2700920 (3035)
Res. (0571) 2742501
E-mail : kml2@rediffmail.com

Dated: 20.10.4

CERTIFICATE

Certified that the dissertation report entitled ***"Analysis and Modeling of Nano Physics Based Devices: (CNTFETs)"*** submitted by ***Mr. Parvej Ahmad Alvi*** is a record of the candidate's own work carried out by him under my supervision and guidance. The results presented in this dissertation have not been submitted elsewhere and are sufficient for submission to the award of ***M. Phil.*** degree.

(Prof. K. M. Lal)
Supervisor

Dr. M. Jawaid Siddiqui
(Reader)

DEPARTMENT OF ELECTRONICS ENGINEERING
Z. H. COLLEGE OF ENGG. & TECH.
ALIGARH MUSLIM UNIVERSITY
ALIGARH-202 002, INDIA
Phone : Off. (0571) 2721148
Res. (0571) 2702923
Fax : 05712721148
Cell : 05713117642
E-mail : mjs_Siddiqui@rediffmail.com

Dated: October 15, 2004

CERTIFICATE

This is to certify that the dissertation report entitled ***"Analysis and Modeling of Nano Physics Based Devices: (CNTFETs)"*** submitted by ***Mr. Parvej Ahmad Alvi*** to the Department of Applied Physics in partial fulfillment of the requirements of the award of ***M. Phil*** is a bonafide record of original work carried out by him under my supervision and guidance.

(Dr. M. Jawaid Siddiqui)
Co- supervisor

ACKNOWLEDGEMENT

Allah, Most Gracious & Merciful, beginning in His Name

First of all I am highly indebted and thankful, the lord of Universe (Allah), the most merciful and benevolent to all, who taught men that which he knew not and bestowed the men with epistemology and gave him the potential to ameliorate the same. It is His blessing, which inspired and enabled me to complete this work.

It is my pleasant duty to acknowledge the help received from several individuals during the work.

I wish to express my profound gratitude, respect and honour to my venerable supervisor, Dr. K.M. Lal, Professor and Chairman, Department of Applied Physics, Faculty of Engineering and Technology, A.M.U., Aligarh for his excellent sprit, illuminative and precious guidance, constant supervision, critical opinion and timely suggestion, constant useful encouragement and technical tips. Without his insistent help and guidance, I would have never been able to complete the report.

I am also indebted to my co-supervisor Dr. M. Jawaid Siddiqui, Reader, Department of Electronics Engineering, Faculty of Engineering and Technology, A.M.U., Aligarh for constant efforts, encouragement and valuable suggestions during the whole period of my dissertations work.

My special thanks goes to Dr. S. Alim H. Naqvi, Professor and Ex-chairman, Department of Applied Physics, Faculty of Engineering and Technology, A.M.U., Aligarh, for his constant co-operation, sympathy, encouragement, suggestion, keen personal interest and scholarly criticism. He enlightened me on various aspect of the study and helped me with his matured suggestions.

Thanks are also due to respected teachers Dr. Alimuddin (Reader), Dr. Ameer Azam, Dr. Shakeel Khan (Lecturers), Department of Applied Physics, Faculty of Engineering and Technology, A.M.U., Aligarh, for valuable support and encouragement.

I earnestly make thanks to my Seniors Dr. Sikandar Ali, Dr. Rajesh Sharma who enlightened me on various aspects of the study.

I would like to thanks my colleagues Mr. Prince Mufti Zia-ul-Hasan, Mr. Jawed Ahmad Rizawi, Mr. S. Asad Ali, and Mr. Parvez Ali for their gregarious nature and timely support encouragement, help and valuable suggestions in completion of this dissertation. The best co-operation received from Mr. Kamal Garg, Mr. Sahabuddin, Mr. Shamsul hasan, and Mr. Rais Ahamd. Infact, merely mentioning names cannot pay thanks but I am grateful to the entire members of the Department of Applied Physics, A.M.U. Aligarh.

I will be failing in my duties if I miss to express my profound and deepest sense of gratitude to my parents and other family members for their keen interest in my studies, manifold assistance, immense support and encouragement without which it was impossible to complete this dissertation.

Last but not least, I would like to thank the Aligarh Muslim University, Aligarh for providing me the facilities.

Place: Aligarh

Date: 10.03.05

Parvej Ahmad Alvi .

C O N T E N T S

Chapter 1

Nanotechnology 1/

Chapter 1

Nanotechnology

1.1 Introduction

Nanoscience and nanotechnology are buzzwords that popup all over the world. We define nanoscience as the study of phenomena and the manipulation of materials at atomic, molecular, and macromolecular scales, where properties differ significantly from those at larger scale, and nanotechnologies as the design, characterization, production, and application of structures, devices, and systems by controlling shape and size at the nanometer scale. These definitions cut across many traditional scientific disciplines and encompass a broad and varied range of materials, tools, and approaches. Indeed, the only feature common to the diverse activities characterized as 'nanotechnology' is the tiny dimensions on which they operate. We have therefore found it more appropriate to refer to " nanotechnologies". Nanotechnology is based on the recognition that particles less than the size of 100nm(a nanometer is a billionth of a meter) impart to nanostructures built from them new properties and behavior [1]. This happens because particles which are smaller then the characteristic lengths associated with particular phenomena often display new physics and chemistry, leading to new behavior, which depends on size.

The first observation was that materials have been and can be nanostructured for new properties and novel performance. The underlying basis for this is that every property of a material has a characteristic or critical length associated with it. For

example, the resistance of a material that results from the conduction electrons being scattered out of the direction of flow by collision with vibrating atoms and impurities, can be characterized by a length called the scattering length. This length is the average distance an electron travels before being deflected. The fundamental physics and chemistry change when the dimensions of a solid become comparable to one or more of these characteristic lengths, many of which are in the nanometer range. So the electronic structures, conductivity, reactivity, melting point and mechanical properties have all been observed to change when particles become smaller than the critical size [1]. This is the basis of the quantum dot, which is a relatively mature application of nanotechnology resulting in quantum-dot laser presently used to read compact disks (CDs).

Nanotechnology is described as a technology to prepare materials using nanosized building blocks (1-100 nm) for making macro size components and devices with better physical, chemical and biological properties when compared to those made from conventional bulk materials – generally known as crystalline, polycrystalline and amorphous materials. Nanosized building blocks in form of nanodot, nanowire and nanosheet having zero, one and two-dimensional structure respectively, involve effectively few tens to few hundreds of atoms and this gives rise to prominent size effect, in case, the excitation wavelength is comparable to the dimension of the nanostructure. This is also termed as quantum confinement effect, which in turn amounts to quantization of excitation interacting with nanostructures. These excitations are basically electrons, holes, phonons, excitons and photons. Size effect may lead to tunable material properties – material properties changing as the size varies. Size effect, associated with the stable material building blocks, if retained in its original form during various stages of material processing steps involving thermal, mechanical and chemical treatments, imparts extraordinary combinations of material properties not expected under normal conditions. It opens up a whole lot of newer possibilities, hitherto unknown, to realize materials with multifunctional

properties caused by nanosized building blocks. Such materials are termed as nanomaterials or nanostructured materials to differentiate them from the usual materials.

There are some examples, in brief, to illustrate extraordinary properties of nanomaterials. Nanostructured metal alloys have very high fracture strength when compared to microstructured counterparts. Nanostructured catalysts are far more efficient and operate at relatively lower temperatures. Super hard surface coating have been successfully developed using nanostructured multiple thin films of hard materials with measured hardness exceeding over that of the diamond - the hardest known material. Semi conducting nanoparticles have tunable discrete energy levels, which could be advantageously used for their enhanced electro optical characteristics such as optical absorption lasing action. Nano laser on a flexible polymer sheet is the future form of laser devices being targeted in the present developments. UV absorption of nanosized titanium dioxide and zinc oxide have been exploited for making sun blocking creams, lotions and cosmetics besides manufacturing wrapping paper for keeping the food-stuff fresh for a longer duration with superior performances. Nanoparticles could be used for targeted drug delivery with controlled drug release at the desired location and lasting over a longer duration. Nanocomposites with variety of polymers are going to revolutionize a variety of industrial engineering applications besides providing better alternatives for human bone structures and other artificial organ transplants. Nanomaterials are found to possess excellent sensing properties as compared to their microstructured and bulk counterparts and therefore a large variety of chemical and biosensors are foreseen to be available soon in the market at very low cost. This will provide very reliable instruments to function like electronic nose and electronic tongue for industrial applications. Laboratory on a chip concept involving micro fluidic structures and appropriate nanosensors will revolutionize the medical diagnostics and human health care sectors to a great extent in very near future. Use of nanomaterials in paints and

other surface coating preparations will provide scratch and corrosion resistant behaviour besides self- cleaning features at low cost and such coating will last much longer than the normal ones. Nanocomposites are being developed with self – repairing or healing characteristics, which will enhance the life of the space vehicles by affecting the on –board repairs during flights and thus the space research will be less costly in future.

1.2 Historical Review

Nanotechnology deals with various structures of matter having dimensions of the order of a billionth of a meter. While the word NANOTECHNOLOGY is relatively new, the existence of functional devices and structures of nanometer dimensions is not new, and infact such structures have existed on the earth as long as life itself. Nature depends fundamentally on nanostructures and processes operating at the nanoscale, from simple colloids such as milk to highly sophisticated proteins. The abalone, a mollusk, constructs very strong shells having iridescent inner surfaces by organizing calcium carbonate into strong nanostrucured bricks held together by glue made of a carbohydrate protein mix. Free nanoparticles also occur naturally as by-products of combustion and cooking. In some sense, nanoscience and nanotechnologies are not new: size dependent properties have been exploited for centuries. For example, Au and Ag nanoparticles (particles of diameter less than 100 nm) have been used as colored pigments in stained glass and ceramics since 10^{th} century AD. Many chemicals and chemical processes have nanoscale features and, for example, chemists have been making polymers-large molecules made up of nanoscalar subunits- for many decades. Nanotechnologies have been used to create the features on computer chips for the past 20 years. However, through the invention of imaging techniques like the scanning tunneling microscope (STM) and the atomic

force microscope (AFM), our understanding of the nanoworld has improved dramatically, and this is leading to an enhanced ability to control structure at the nanoscale.

It is not clear when human first began to take advantage of nanosized materials. In the fourth-century A.D. Roman glassmakers were fabricating glasses containing nanosized metals. A cup (called *licurgus cup*) was made from soda lime glass containing gold and silver nanoparticles. The color of the cup changes from green to deep red when a light source is placed inside it. Photography, a mature and advanced technology has been developed in eighteenth and nineteenth century, which depends on production of silver nanoparticals sensitive to light. So technology based on nanosized materials is really not that new.

- In 1956, Uhlir reported first observation of porous Si having pores of nanometer dimensions. The porous Si was fluorescent at room temperature.
- In 1960s, Magnetic fluids called *Ferrofluids* were developed, which consist of nanosized magnetic particles dispersed in liquids.
- In 1965, a great scientist Richard Feynman envisioned building circuits on nanoscale that could be used as element in more powerful computers.
- In1970s, First time two-dimensional quantum wells were developed by IBM and Bell laboratories.
- In 1980s, appropriate methods of fabrication of nanostructures were developed.
- In1985, A fullerene molecule (C_{60}) was synthesized.
- In 1986, the scanning tunneling microscope (STM) was developed by G.K. Binning and H.Roher at IBM laboratory and the were awarded the Nobel Prize for this. STM is an important tool for viewing, characterizing and atomic manipulation of nanostructures.
- In 1990s, Sumio Lijima made carbon nanotubes (CNTs), and superconductivity and ferromagnetism were found in C_{60} structures.

- In 1996, CNTFETs have been demonstrated using carbon nanotubes in place of channel between source and drain electrodes in the ballistic MOSFETs.

1.3 Applications, Developments, And Opportunities

A large number of potential applications of nanotechnologies are now opening up. Much of nanoscience and nanotechnologies are concerned with producing new or enhanced materials. Some nanotechnology-enabled products are already on the market and enjoying commercial success. For example, self-cleaning windows use a 15 nm thick coating of activated TiO_2 engineered to be highly water-repellent, so that rainwater just flows off the surface, washing away the dirt. Nanoparticles are used in some sunscreens to reflect and absorb ultraviolet (UV) light.

Future applications of nanomaterials include lighter, stronger materials, the use of nanoparticles to clean up contaminated land, and nanoengineered membranes for more energy-efficient water purification or desalination.

Computer chips and CD and DVD drives are already operating at nanoscales, and nanoscience and nanotechnologies will continue to have a pivotal role in the progressive miniaturization of computer chips and the enhancement of data storage. There is also a huge impetus to develop alternative technology and materials to Si. For example, plastic electronic devices, using conducting polymers for data storage and transfer, are cheaper to manufacture than Si-based devices, and will be particularly suitable for inexpensive applications like smart cards, where speed and high memory capacity are less critical. It could also enable advances such as roll-up TV screens.

Nanotechnology are also enabling the development of smaller, cheaper sensors, which will have a wide range of applications from monitoring the pollution in the environment, the freshness of food, or the stresses in a building or a vehicle.

Much interest is also focused on quantum dots, which are semiconductor nanoparticles that can be 'tuned' to emit or absorb particular colors of light for use in solar or fluorescent biological labels.

Applications of nanotechnologies in medicines are especially promising in the longer term. These can be expected to enable drug delivery targeted at specific sites in the body so that, for example, chemotherapy is less invasive. Nanotechnology is expected to lead to stronger, longer-lasting implants; sensors that can be used to monitor various aspects of human health; and provide improved artificial cochleae and retinas. However, many of these applications will not be realized for at least ten years, partly because of the rigorous testing and evaluation that will be required. Antimicrobial wound dressing are already on the market in the USA. These use nanocrystalline Ag to provide a steady dose of ionic Ag to protect against secondary infections and are claimed to be effective against 150 different pathogens.

An interesting aspect of the current decade for nanotechnologies is that, for the first time, there is a convergence between the two approaches to creating nanostructures, particles, and the systems. Top-down manufacturing, perfected by the semiconductor industry over the last 30 years, involves precision engineering and lithography to grind or cut bulk materials into tiny pieces and to etch or print nanoscale patterns onto them. Bottom-up manufacturing assembles nanostructures from scratch through conventional chemical synthesis, self-assembly (chemical bonding to assemble structures, like crystal formation), and positional assembly (where atoms or groups are manipulated individually into a structure). The two approaches can now control product dimensions of a similar order, which opens up exciting new possibilities in hybrid manufacturing.

Materials can behave quite differently at the nanoscale to the way they do in bulk. This is both because the small size of the particles dramatically increases surface area and therefore reactivity, and also because quantum effect start to become significant. This potential difference is just what makes them interesting to scientists.

However, it also means that their toxicity may be different from that of the same chemical in the form of larger particles. There are examples where nanoparticles can produce toxic effects even if the bulk substance is nonpoisonous. This arises partly because they have increased surface area and also because, should the nanoparticles enter the body through inhalation, or absorption through the skin, they are able to move around and enter cells more easily than the larger particles. It is very unlikely that new, manufactured nanoparticles could be introduced into humans in doses sufficient to cause the health effects that have been associated with air pollution. Another area of potential exposure to nanoparticles is through the use of some cosmetics and sunscreens. For example Fe_2O_3 nanoparticles are used as a base in lipsticks. Nanoparticles of TiO_2 and ZnO are already in use in certain sunscreens, as they absorb and reflect UV radiations, but are also transparent on the skin. Studies so far on TiO_2 nanoparticles suggest that they do not penetrate the skin. However, as both cosmetics and sunscreens they are intended for use on undamaged skin. Thus, nanoparticles and nanomaterials continue to attract a great deal of attention because of their potential impact on an incredibly wide range of industries and markets.

1.4 Nanotechnology In Carbon Materials

Carbon is unique material from the standpoint of Nanotechnology. It can be a good metal in the form of graphite, a wide gap superhard semiconductor in the form of diamond, a superconductor when intercalated with appropriate guest species, or a flexible polymer when reacted with hydrogen and other species. Furthermore, carbon-based electronic materials provide examples of materials showing the entire range of dimensionalities from fullerenes which are 0D quantum dots, to carbon nanotubes

which are 1D quantum wires, to graphite which is a 2D layered anisotropic material, and finally to diamond, a 3D wide gap semiconductor [2].

With in this family of electronic materials, fullerenes and carbon nanotubes are the newest additions and are the subject of study. In the preparation of fullerenes by any of the conventional synthesis methods (by carbon arc discharge, laser pyrolysis, or combustion flames) the fullerene species of greatest abundance by far is C_{60}, the most stable of the fullerenes and the fullerene with greatest symmetry. All C_{60} molecules are identical and can be synthesized to high purity and in large quantities (gram quantities) at relatively low cost, the C_{60} molecule is attractive for a variety of nanostructure applications.

Carbon nanotubes have great potential for nanoscale electronic applications because of their small diameter and versatile electronic properties. Since carbon nanotubes are considered as 1D quantum wires, it is possible to utilize nanotubes for nanowire applications in interconnecting nanoscale devices. By varying the chirality and diameter of carbon nanotubes, it is possible to alter the properties of the nanotubes from metallic to semiconducting. Such nanotubes could, in their own right, lead to nanoscopic electronic devices based on concentric semiconducting and metallic carbon tubules. Because the nanotubes themselves do not require any doping by impurities, as conventional semiconductors do, but acquire their electronic properties from their geometry, the resulting devices should be highly thermally stable and have high intrinsic mobility.

While the field of nanotechnology based on carbon nanotubes is still about half way between science and science fiction, it is a very active fast growing field whose promise of nanoscale molecular devices and orders of magnitude increase in the integration density of electronic components is too appealing to be ignored. The discovery of fullerenes has given a significant boost to the field of nanotechnology by providing an abundance of stable, highly symmetric, non-reactive, and relatively large molecules that can, in principle, be manipulated one at a time. Fullerenes at

semiconductor interfaces can be utilized to modify electronic device behavior on nanometer length scales. Together with other carbon structures, a new carbon based nanotechnology can be envisioned.

Although fullerenes and nanotubes share many common features, their differences regarding structure and properties are sufficiently large. The structure and properties of fullerenes and carbon nanotubes are reviewed in the next chapter in the context of nanotechnology.

1.5 Nanotechnology In Electronics (Nano-Electronics)

In nanotechnology a new frontier exists on the head of pin. On this frontier classical laws of physics that govern the mechanics of our common experience are suspended. The exploration of this frontier was spawned by the integrated circuit (IC) revolution and the requirements of miniaturization that make ICs possible. ICs now pervade our lives and have enabled space flight, the information age, and that toasters that get it right every time. Moreover, the same techniques used to integrate and manufacture electronics have provided us with the opportunity to fabricate micro machining and micro robots. The requirements of miniaturization, micro machining and integration are becoming more stringent as the minimum feature size (MFS) shrinks. For example, a Pentium® processor is comprised of about 4-million electronic switches, and each switch is only a few thousand atoms long. Devices this small are shorter than the wavelength of visible light, and consequently the conventional means for producing them, which employs optical lithography as a key element, can not be inexpensively extended to much smaller scales. Following the evolutionary development of technology, there have been numerous forecasts of a small wall near an MFS of 100 nm, beyond which conventional IC technology will stall because of the cost of fabrication [3,4]. Yet, there is still no consensus on a

revolutionary, inexpensive route for producing smaller features to breach this wall. An economical route to feature size 100 nm and smaller has been a primary motivation for research on the nm frontier.

The transistor was invented in 1947 [5] for use as an amplifier and electronic switch. The invention grew in economic importance as it became a smaller, lower power, more reliable alternative to the mature vacuum tube technology, but for many years it showed lower performance and often at higher cost than the earlier technology. So, the transition was slow. We often talk about the revolution caused by the invention of the transistor, but, infact, there was a relatively gradual evolution that continued for decades: eg. The development of Si BJTs with a diffused emitter and base [6], followed by the development of plane Si transistors [7] and the MOSFET [8,9]. Thus, transistor became the cornerstone of modern computation and communications, not because it caused a revolution in electronics, but because it enabled the development of the integrated circuit (IC). The growth in complexity of Si IC technology as measured by number of transistor in a DRAM (dynamic random access memory) is shown in Figure 1.

Moore's law follows this astounding trend in complexity, which states, "The number of transistors incorporated on a memory chip doubles every year and a half" [10]. This has resulted from continual improvements in design factors such as interconnectivity efficiency, as well as from continual decreases in size. Economic considerations driving this revolution are the need for more and greater information storage capacity, and the need for faster and broader information dispersal through communication networks. Another major factor responsible for nanotechnology revolution has been the improvement of old and the introduction of new instrumentation system for evaluating and characterizing nanostructures.

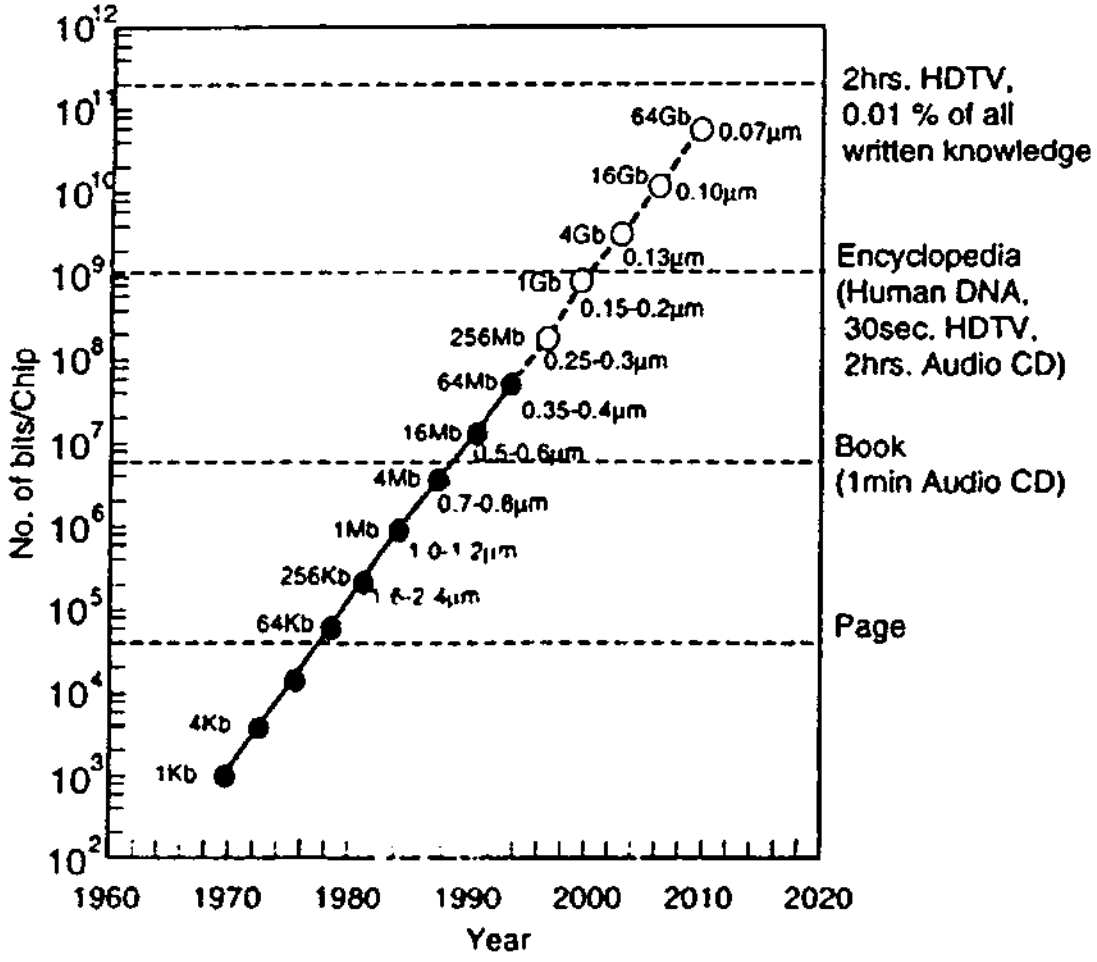

FIGURE 1. The complexity curve adapted from Moore showing the development in time of the information storage capacity of silicon DRAM chips.

An important impetus that caused nanotechnology to advance so rapidly has been the development of instrumentation such as the scanning tunneling microscope (STM) that allows the visualization of the surfaces of nanometer-sized materials. Developments of large –scale inexpensive methods of fabrication is major challenge for nanotechnology if it is to have an impact on technology.

1.6 Chemical Approaches In Nanotechnology

At present "nanotechnology" is a vision rather than a reality. We do not have practical, manufacturable methods to make complex materials, machines, and electrical circuits on the 1-100 nm scale. However, there is a flourishing "Nanoscience" research effort involving ideas and methods drawn from chemistry, physics, and engineering science. "Nanoscience" presently is in a discovery stage, uncovering new physical processes and effects, and learning how to implement these processes in new devices and designed materials. The key technological issue is control of natural processes to make assemblies of nanometer components in useful ways.

The 1-100 nm "nanoscale" length is intermediate between the traditional realms of synthetic chemistry, and VLSI lithographic processing as employed in electronics. The two main approaches to nanoscience, colloquially "bottom-up" and "top-down", represent extensions of these methods, respectively, into the intermediate territory.

The "top-down" approach uses lithography (e-beam, x-ray) or scan probe methods (AFM, STM) to create and explore nanometer structures. This approach to the preparation of nanostructures starts with a large-scale object or pattern and gradually reduces its dimension or dimensions. This can be accomplished by lithography technique, which shines radiation through template on to a surface coated

with a radiation-sensitive resist; the resist is then removed and the surface is chemically treated to produce the nanostructure.

The "bottom-up" approach develops chemical synthetic "self-assembly" methods to create and explore nanostructure. This approach to the preparation of nanostructure is to collect, consolidate, and fashion individual atoms and molecules into the structure. This is carried out by a sequence of chemical reactions controlled by catalysts. It is a process that is widespread in biology where, for example, catalysts called enzymes assemble amino acids to construct living tissue that forms and supports the organs of the body. This explains how nature brings about this variety of self-assembly.

One might suspect that, as object and devices decrease in size to tens and hundreds of atoms in diameter, chemical ideas and methods must become useful and efficient. For example, the semiconductor nanocrystals synthesis that is most highly developed, and closest to being a useful methodology, is the organometallic synthesis of *CdS* and *CdSe*, both II-VI semiconductors with sp^3 tetrahedral bonding and direct band gaps in the visible. In favorable cases, high quality semiconductor nanocrystals with controlled surfaces can be made in gram amounts, and can be used as building blocks for new materials and devices. Nanocrystals are also used to explore the size dependence of electronic, optical, and structural properties.

In the context of nanotechnology, semiconductor nanocrystals are building blocks. Size and choice of material determine the optical and electrical properties, while surface chemistry determines charge transfer and electron-hole recombination kinetics. The quantum mechanics of three-dimensional confinement is now moderately well understood. The semiconductor nanocrystals (such *CdSe*) family shows the potential of chemical synthesis to create gram amounts of high nanocrystals, with chosen and variable surface chemistry [11]. With in ten years all major semiconductors should be available at this level of precision and quality.

1.7 From The Bottom Up: Building Things With Atoms

The revolutions in the electronics industry and the chemical and drug industries have been brought about by an ability to build two kind of small things: molecules and electronic circuits. The challenge faced by the electronics industry is opposite to that faced by the chemical and drug industries. While the electronics industry strives to build ever-smaller circuits, the chemical and drug industries strive to build ever larger and more complex molecules. The electronics industry makes its circuits in a top down approach using lithographic techniques to whittle circuits out of a block of silicon, while the chemical and drug industries use the bottom up approach of swirling together chemical sub-units in such a way that huge numbers of the desired molecule or product are ultimately created.

Atom manipulation was made possible by the invention of a most remarkable and versatile instrument: the scanning tunneling microscope, or STM for short [12]. The STM is an instrument capable of creating atomic resolution images of the surface of electrically conducting materials such as metals and semiconductors.

Just as the blind person can sense not only the shape of the object, but also its texture, compressibility and thermal conductivity, the STM can tell us much more about a surface than just its shape. We can use it to study how the electrons in the near- surface layer have arranged themselves not only spatially, but also energetically. Even more remarkable, just as the blind person can push, pull, pick up and put down objects on a table top, so too can we push, pull, pick up and put down surface atoms using the tip of the microscope. Here is how it is done.

In figure 2(A) we see a schematic illustration of an atom, which lies on top of a metal surface. The forces, which hold the atom to the surface, are due to the chemical binding of the atom to the nearby atom of the surface. These forces are schematically represented by springs shown in figure 2. To image this atom the tip is scanned over

the surface, following a trajectory shown by the dashed line in figure 2(A). Under these conditions the separation between the tip and the atom on the top of the surface (called an "adatom") are great enough so that any forces between the tip and the adatom are negligible, the result being that the adatom will hold still to have its picture taken.

Just as there are chemical binding forces between the adatom and the nearby atoms of the surface, there will a chemical binding force between the adatom and the outermost atom(s) of the tip. In Figure 2(B) we have schematically represented the chemical bonding interaction between the tip and the adatom as a spring. This is called "tunable bond" because both the direction and the magnitude of the force exerted on the adatom can be tuned simply by adjusting the position of the tip. Now it turns out that for a wide range of adatom, and even for groups of adatom or molecules, it is possible to adjust the height of the tip so that in-plane force exerted by the tip on the adatom is great enough to overcome the in-plane forces between the adatom and the underlying surface, yet at the same time the out of plane force exerted on the adatom by the tip is not so great as to overcome the out-of-plane forces between the surface and the adatom. When these conditions are achieved, it is possible to move the tip sideways and drag the adatom along the surface. This process, called the sliding process, allows one to position adatoms with atomic scale precision. The trick is to be able to successfully switch between operating the microscope in an imaging mode with the tip at a height where its interaction with the adatom is negligible, to operating the microscope in the manipulation mode with the force between the tip and the adatom sufficient to drag the adatom along the surface under the tip. The sliding process [13] is indicated in Figure 3.

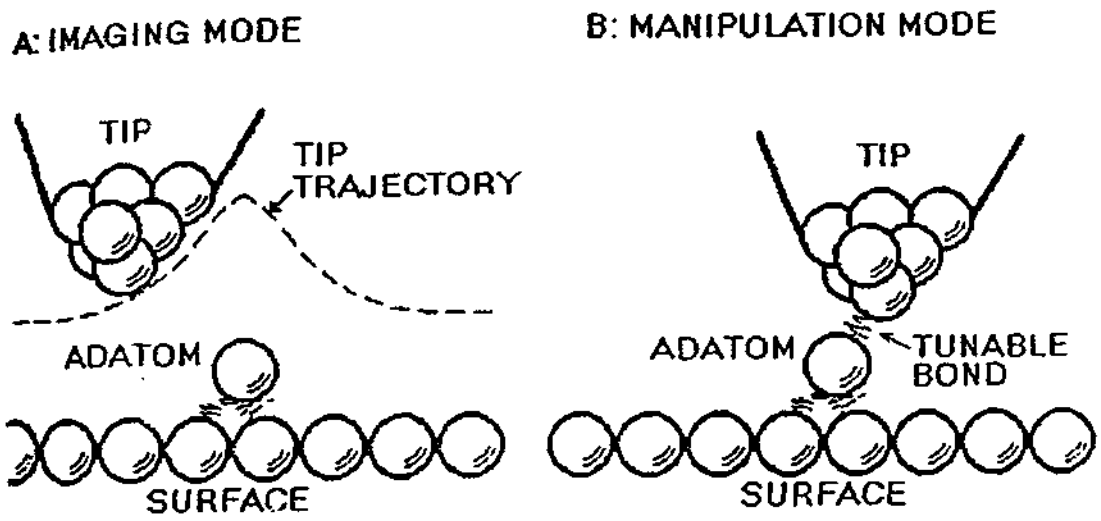

FIGURE 2. (A) In the imaging mode the tip is stabilized far enough above the surface so that the interaction between the tip and the adatom is negligible. (B) In the manipulation mode the tip is brought close enough to the adatom to drag the adatom along the surface. The force exerted on the adatom by the tip is due to the partially formed chemical bond between the tip and the adatom.

In order for the sliding process to work correctly, it is best to use combinations of adatoms and the surfaces where the lateral, or in-plane, interaction between the adatom and the surface is not too great. The week in plane interaction between adatom and surface means that very little thermal shaking of the adatom would be required in order for the adatom to spontaneously hop from site to site across the surface, that is, to undergo thermal diffusion. Thermal diffusion is generally undesirable because it causes the randomization of the location of adatom, thus destroying the work of placing the adatom at particular locations.

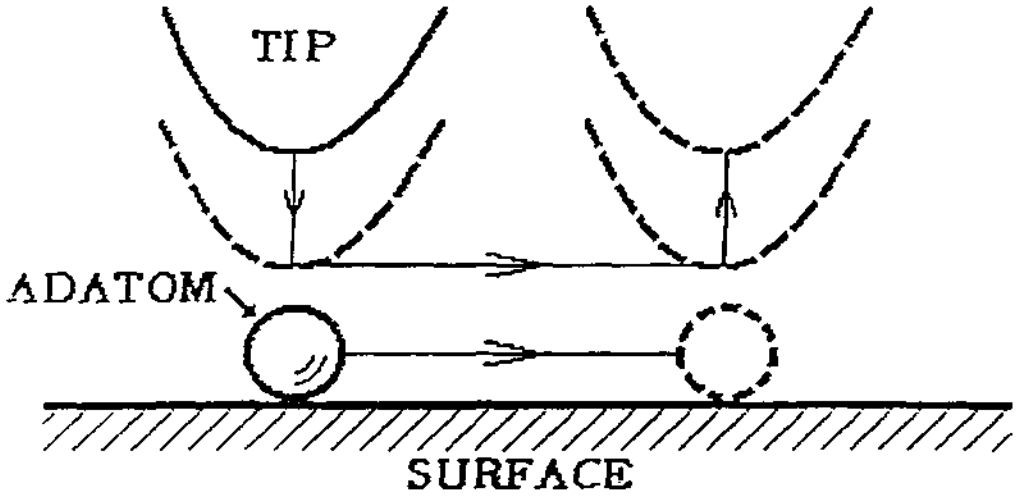

FIGURE 3. Schematic of the sliding process. The tip is placed above the adatom and then lowered to an empirically determined height at which the attractive interaction between the tip and adatom is sufficient to pull the adatom along the surface. Once the adatom is moved to its final location, the tip is raised back to the height used for imaging, effectively terminating the tip-adatom interaction.

The solution to this problem is to conduct the experiment at low enough temperature that the rate of thermal diffusion is very slow compared to the duration of the experiment. This can be achieved by cooling the sample and the tip of the microscope to the temperature of liquid helium, some to 269 degrees centigrade below the freezing point of water. Cooling to liquid helium temperature introduces some complication in the design of the apparatus, but it brings with it a variety of advantages relative to the overall performance of the STM. The STM is contained in a vacuum vessel, which is designed to provide a degree of vacuum sufficient to maintain the surface of a sample clean for weeks at a time (a metal surface exposed to atmospheric pressure would be contaminated with a monolayer of gas molecules in about one microsecond, thus the need for so called " Ultra-High Vacuum"). In addition, the chamber, which houses the microscope, and everything with in that

chamber, is cooled to liquid helium temperature for the above-mentioned reasons. The application of atom manipulation for technological purposes is, at the moment, far beyond sensible consideration. On the other hand, it is likely that in the years ahead atom manipulation will be heavily exploited as a scientific tool.

At present we have no concept of how to assemble nanocrystals into a complex, designed circuit, with anything like the generality of present micrometer scale lithographic silicon technology. Infact we need to convince ourselves that this is a practical and worthwhile goal on the nanometer scale. Over long time scales, unexpected discoveries can change human perspective on the importance and relative priority of such heroic tasks. Last time it has been realized that "quantum computation" offers a major scaling advantage in parllel processing, when compared with macroscopic computer algorithms [14]. "Quantum computation" conceptually operates by coherent wave function propagation in a microscopic system. Loosely speaking, nature herself does the computation. Perhaps some new idea such as this will provide the momentum necessary for a major assault on creation of a practical nanotechnology. Somehow, physics, chemistry and electronics manufacturing will ultimately merge on the nanometer scale.

Final Remark

Nanoscience and nanotechnologies offer great opportunities. Almost all nanotechnologies pose no risks to health or the environment. In the longer term, it is hoped that nanotechnologies will enable more efficient approaches to manufacturing using less raw materials and energy. However, we have concerns about manufactured nanoparticles and nanotubes that are in a form where they are free to interact with humans or the environment.

References

1. Charles, P. Poole, Jr. and Frank J. Owens, "Introduction to Nanotechnology", 2003.
2. Dresselhaus, M.S., Dresselhaus, G., and Saito, R., "Nanotechnology in carbon materials", in Nanotechnology, G.Timp, ed., Springer-Verlag, 1998, chapter, p.285.
3. Hutcheson, G.D. and Hutcheson, J.D., Scientific American 274, 54-63 (1996).
4. Stix, G., Scientific American 272, 90-95 (1996).
5. Bardeen, J., and Brattain, W.H., Phys. Rev. 74, 230-231 (1948); Schockley, W., Bell Syst. Tech. J.28, 435-439 (1949); Schockley. W., Proc. IRE 41, 970 (1953).
6. Tanebaum, M., and Thomas, D.E. Bell Syst. Tech. J. 35, 1(1956).
7. Hoerni, J.A., " Planar Silicon Transistor and Diodes" IRE Electron Devices Meeting, Washington, D.C. 1960.
8. Atalla, M.M., Patent, V.S., 3, 206, 670 (filed in 1960, issued in 1965).
9. Kahng, D., and Atalla, M.M. IRE-IEEE Solid-State Device Research Conference, Carnegic Institute of Technology, Pittsburgh, P A, 1960; Kahng, D., U.S. Patent 3, 102, 230 (filed in 1960, issued in 1963).
10. Moore, G.E., IEEE IEDTM Tech. Dig. 11-13, (1975).
11. Louis Brus, "Chemical approaches to Semiconductor Nanocrystals and Nanocrystal materials", in Nanotechnology, G.Timp, ed., Springer-Verlag, 1998, chapter, p.257.
12. Binning, G. and Rhorer, H., Sci. Am. 253, 50 (1985), Hansma, Paul K., J. Appl. Phys. 61 (2), R1 (1987).

13. The sliding process is one of several processes that may be used to manipulate atoms on surfaces with the STM. See Stroscio, J.A. and Eigler, D.M. science 254, 1319 (1991).
14. Shor, P.W., Proceedings of 35th Annual symposium on fundamental computer science, IEEE computer science (Nov. 1994), p.124.

Chapter 2

SPMs – The Scanning Probe Microscopes

Chapter 2

SPMs – The Scanning Probe Microscopes

Nanotechnology is the manipulation of matter on the scale of billionth of a meter and aims at building things with atoms and molecules mimicking Nature's style. Nanotechnology is strongly driven by the SPMs with whom the nano-scale investigation and exploitation becomes possible. Presently there are about two dozen variations of SPMs but the most basic and important of these microscopes are STMs, the scanning tunneling microscopes and AFMs, the atomic force microscopes.

Though the basic concepts of Nanotechnology were propounded by Feynman [1] in 1959, the nanotechnological activities gathered momentum during the period 1980-1990 in which four major breakthroughs occurred. The STM was invented in 1981, the real quantum dot, the C_{60} fullerene was caged by H. Kroto and R. Smalley [2] in 1985, the Atomic Force Microscope (AFM) was built, again, by Binnig and his colleagues [3] in 1985 and in 1990, Sumio Iijima [4] discovered the wonder material, the carbon nanotubes (CNTs). Of these four major nanotechnological events, the inventions of STM and AFM have been of extreme significance because they provided the much-needed nano-vision.

A. Scanning Tunneling Microscopy (STM)

The STM was first developed at the IBM Zurich Research Laboratory in Switzerland by Gerd Binnig and Heinrich Rohrer [5] in 1981. At that time STM was the first microscope, which could give 3-D images of electrically conducting surfaces with resolution in the nanometer range.

Originally Binnig and Rohrer were interested in electrical properties of thin insulating layers and building a microscope was not included in their programme. It was during a discussion on arranging tunneling contacts that Binnig thought of vacuum tunneling which he then took seriously. Binnig along with Rohrer worked ceaselessly to achieve the experimental success whose dimensions were unknown to them. They took couple of weeks to realize that scanning via tunneling would deliver topographical images with atomic accuracy i.e. a new type of microscope was in their hands. They perfected the technique and gave the name Scanning Tunneling Microscope (STM). Strangely, as the arrival of STM was unbelievable, many scientists thought that Binnig & Rohrer's results were mere computer simulations!

2.1 Principal of STM

It is well known that a quantum mechanical wave has finite probability of tunneling through a thin energy barrier even though the height of the barrier is more than the energy of the wave. Initially, quantum tunneling through thin insulating layers was studied by several workers but the idea of Binnig became an unprecedented success story when he removed the atomic thin insulating barrier by vacuum.

The principle of a STM is illustrated in the following Figures:

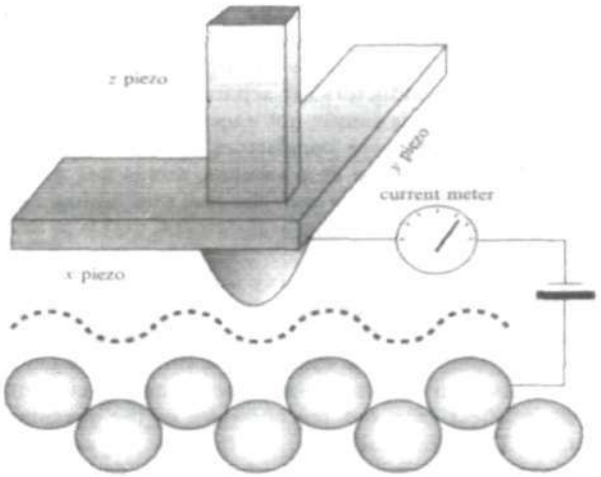

Figure 1. Illustration of scanning of metal tip over the surface under study.

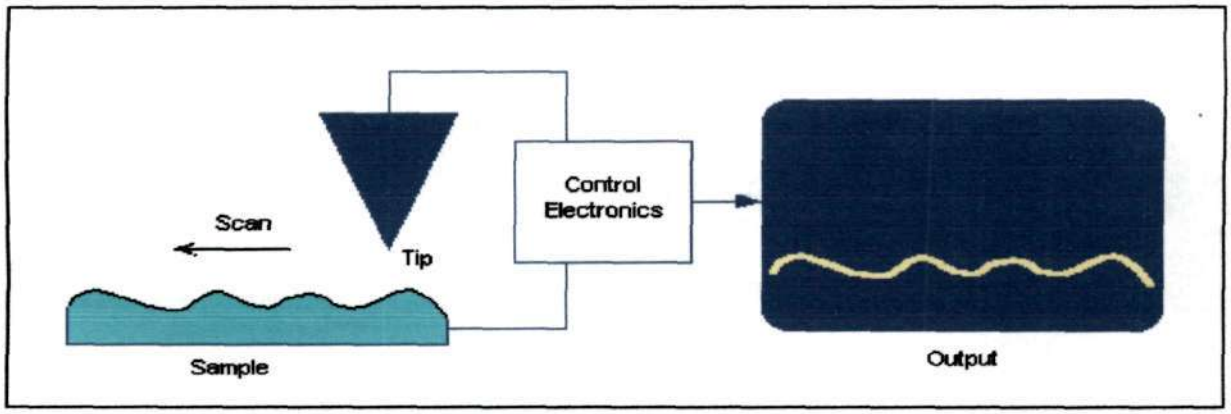

Figure 2. Illustration of scanning of metal tip over the surface with output.

2.2 How Does A STM Work?

The STM is an instrument capable of creating atomic resolution images of the surface of electrically conducting materials such as metals and semiconductors. However, unlike optical microscopes and their cousins the electron microscopes, the STM does not rely upon wave optics to form an image. Incongruously, it forms an image in a way that is similar to the way a blind person can form a mental image of an object by feeling the object. The STM achieves this feat by scanning a metal needle, called the "tip", across a surface while maintaining the tip with in a few atomic diameters of the surface (see Figure 1). This is done by making an electric current flow between the tip and the surface to be imaged. The magnitude of this electric current is very sensitive to the separation between the tip and the surface and thus can be used as a signal for stabilizing the height of the tip as the tip is moved laterally across the surface, as shown in Figure 2 and 3.

By scanning the tip in a raster pattern over the surface and recording the height of the tip, an image of the topography, or shape, of the surface can be recorded. Actually the STM tip is positively charged and acts as a probe when it is lowered to a distance of about 1nm above the surface under study.

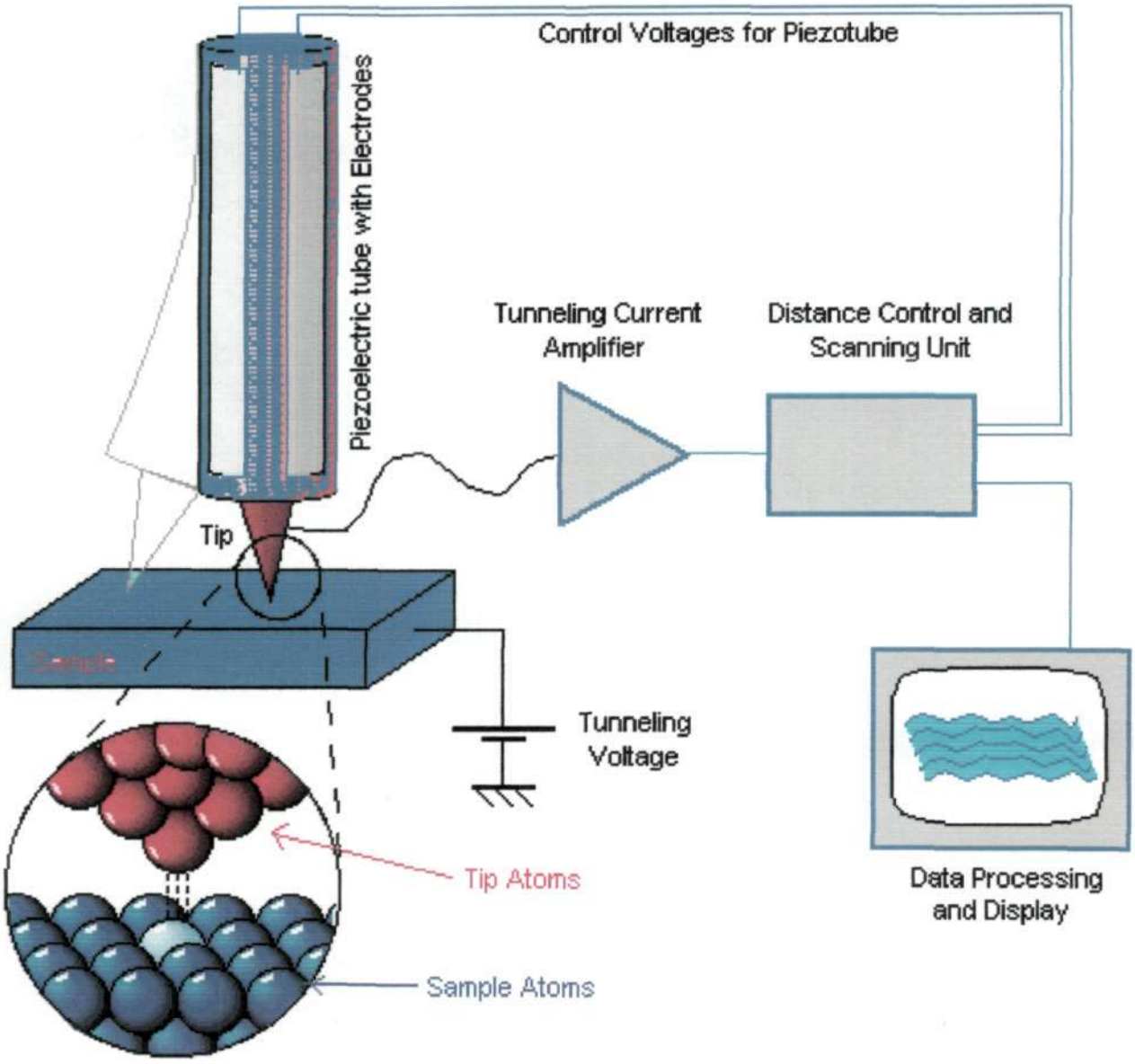

Figure 3. Schematic diagram of STM with electronic circuit.

Electrons at individual surface atoms are attracted to the positive charged of the probe wire and jump (tunnel) up to it, thereby generating a weak electric current. The probe wire is scanned back and forth across the surface in a raster pattern, in either a constant height mode, or a constant current mode, see Figure 4,5 [6].

The principle of electron tunneling is quite old and was given by Giaever [7] in 1960. Binnig and Rohrer studied the electron tunneling through an empty space barrier with the two conductors being separated by nearly an atomic diameter such that there is not enough room for any atom to enter in between the conductors. The electron tunneling together with lateral scanning provides surface images with an extraordinary resolution of less than 0.1 nm.

In an actual experimental setup, a sharp metal tip acts as probe and a tunneling current is produced when the tip is brought close to the conducting surface to be investigated, the separation being $\leq$ 1 nm. The magnitude of the tunneling current depends on the distance between the probe tip and the specimen and therefore the motion of the probe tip thus maps the contours of the specimen surface with atomic resolution. For this purpose the probe has to be moved in a very accurate and precise manner which is achieved by utilizing piezoelectric properties of the crystals whose physical dimensions change by varying voltage applied across the opposite faces. The probe tip may be moved back and forth across the surface in raster fashion in three alternative ways:

(i) Constant height mode
(ii) Constant current mode, and
(iii) Manipulation mode

2.3 Constant Height Mode

In the constant probe height mode the tip is constantly changing its distance from the surface, and this is reflected in variations of the recorded tunneling current as the probe scans (see Figure 4). The feedback loop established the initial probe height, and is then turned off during the scan. The scanning probe provides a mapping of the distribution of the atoms on the surface.

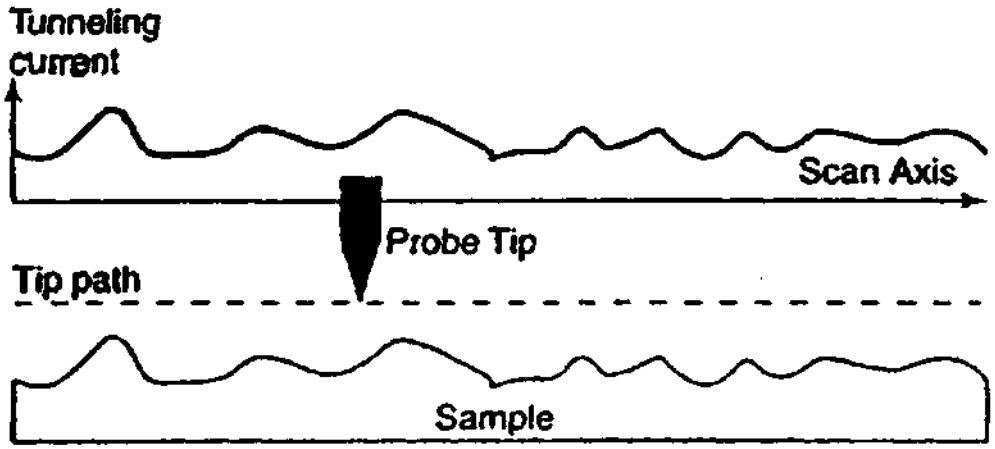

FIGURE 4. Constant height imaging mode of a STM.

2.4 Constant Current Mode

In the constant current mode the height of conducting tip above the sample surface is kept constant at each location, and the up / down probe variations are recorded. This mode of operation assumes a constant tunneling barrier across the surface (see Figure 5).

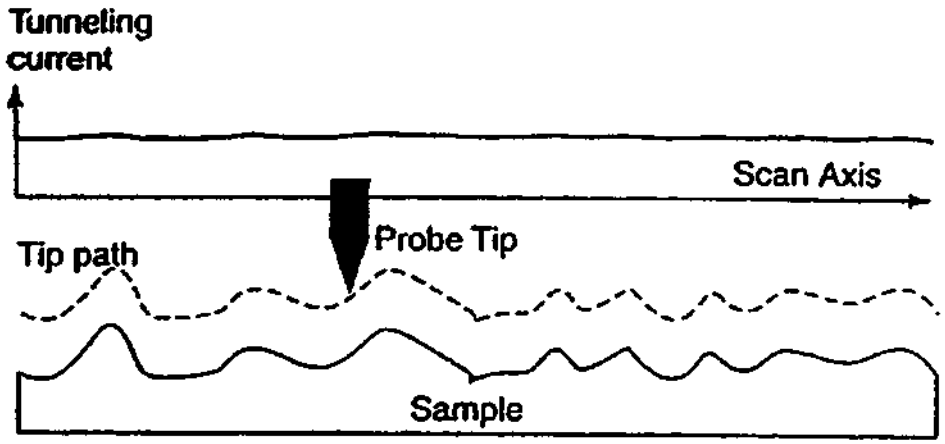

FIGURE 5. Constant current imaging mode of a STM

2.5 Manipulation Mode

STM can be used for atom manipulation, which was accidentally discovered by Don Eigler and Paul Weiss [8] while studying the adsorption and ordering of Xenon on a platinum surface. They found that the probe tip might be used to control the position of an atom on the top of the surface (called "adatom").

In the manipulation mode the tip is brought close enough to the adatom to drag the adatom along the surface. The force exerted on the adatom by the tip is due to the partially formed chemical bond between the tip and the adatom.

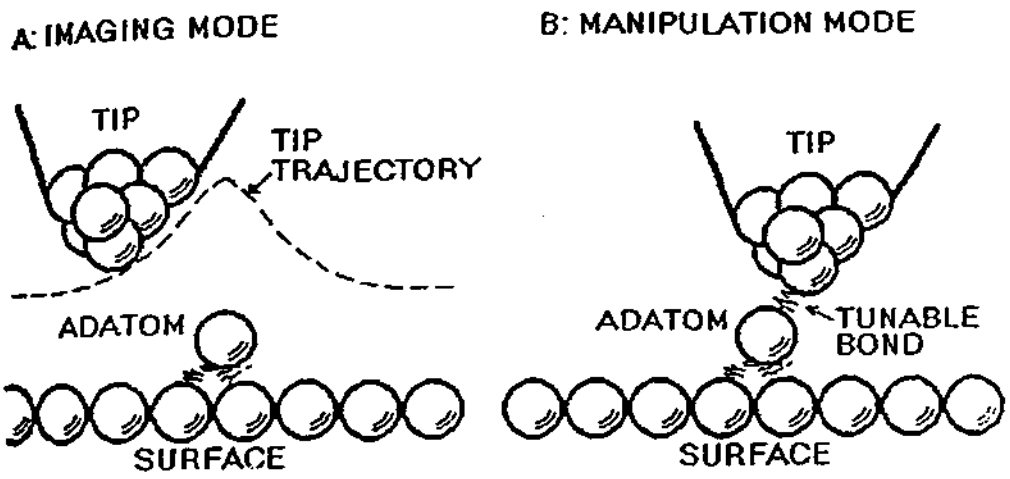

Figure 6. Dragging of adatom along the surface in manipulation mode by STM.

Just as the blind person can sense not only the shape of the object, but also its texture, compressibility and thermal conductivity, the STM can tell us much more about a surface than just its shape. We can use it to study how the electrons in the near-surface layer have arranged themselves not only spatially, but also energetically. Even more remarkable, just as the blind person can push, pull, pick up and put down objects on a table top, so too can we push, pull, pick up and put down surface atoms using the tip of the microscope. Here, how it is done, is shown in Figure 6.

In the manipulation mode, the force between the tip and the adatom becomes large enough to move the adatom along the surface and place it at the desired location. Eigler et al utilized this knowledge to demonstrate the ability to assemble molecules from their constituent atoms. Thus with STM they proved the bottom-up construction as predicted by Feynman was indeed a reality! They further demonstrated the capability

of atom manipulation by constructing a molecule made of eight cesium and eight iodine atoms by bringing one atom at a time by STM (see Figure 7). Eigler et. al.[9] indeed produced first time the sophisticated and beautiful structure which they called a "Quantum Corral" made from 96 iron atoms carefully positioned on a copper surface (see Figure 8). However, with the present level of knowledge, Eigler feels that mass manufacturing by this method in foreseeable future is completely ridiculous.

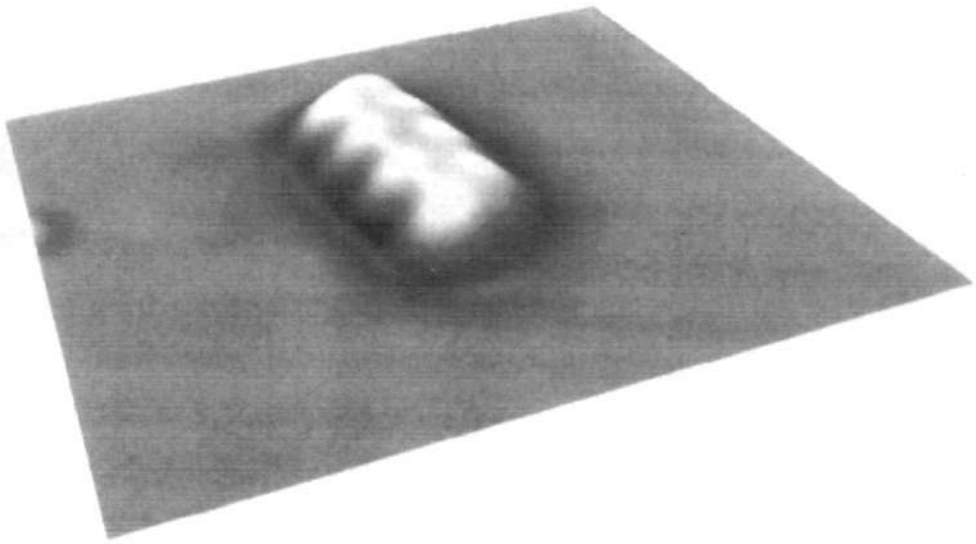

Figure 7. A molecule made of eight cesium and eight iodine atoms constructed by a STM taking one atom at a time.

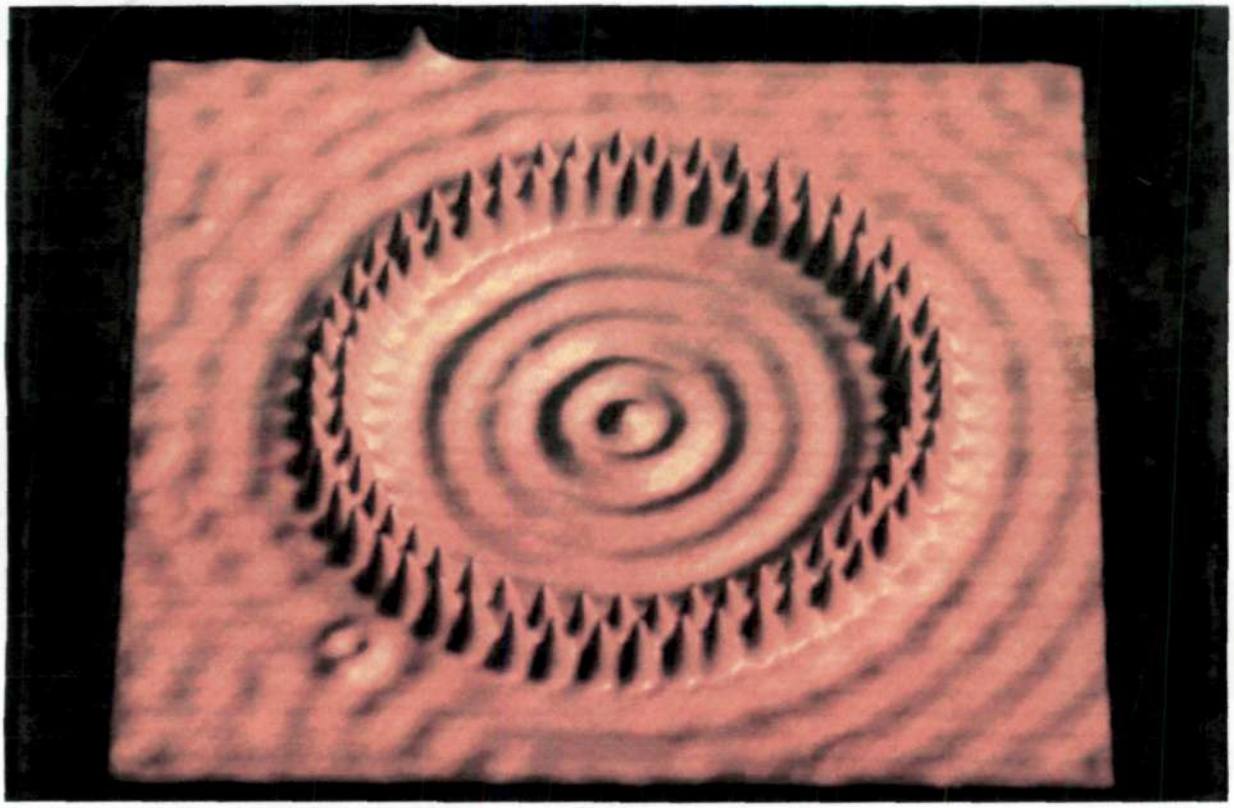

Figure 8. A quantum corral made from 96 Iron atoms on Copper surface (Don Eigler, IBM).

2.6 The Tunneling Current In STM

The STM often employs a piezoelectric tripod scanner. A piezoelectric is a material in which an applied voltage elicits a mechanical response, and the reverse. An applied voltage induces piezo transducers to move the scanning probe (or the sample) in nanometer increments along the x, y or z directions. The tunneling current, which varies exponentially with the probe surface atom separation, depends on the nature of the probe tip and the composition of the sample surface. From a quantum mechanical point of view, the current depends on the dangling bond state of the tip apex atom and on the orbital states of the surface atoms.

The tunneling current, J, in a STM is related to the voltage, V, applied between the specimen and the probing tip by the following relation:

$$J = \frac{q^2 V \chi}{2\pi h l \delta}$$

$$\text{when } \delta = \frac{h/2\pi}{\sqrt{2 m_o (E_{pot} - E_{kin})}} \approx 10^{-9} \text{ m}$$

where q = electronic charge

l = width of the barrier

χ = transmission coefficient

δ = characteristic length for tunneling

$(E_{pot} - E_{kin})$ = extraction energy of an electron

B. Atomic Force Microscopy (AFM)

Next to STM the most widely used technique in nano-technology is the atomic force microscope, which is different from STM in two important aspects. Where as a STM scans the surfaces with the help of tunneling current between the probe tip atoms and the surface atoms, the AFM on the other hand develops the images of the surface by measuring the ultra small forces (less than 1 nN) between the surface atoms and the probe. The AFM in a sense is improvement over STM that it does not require the specimen to be electrically conducting where as in STM both probe tip and the specimen surface have necessarily to be of conducting materials.

In 1985, Gerd Binnig together with two other colleagues Ch. Gerber and C.F. Quate developed AFM, the atomic force microscope, which does not require the specimen to be electrically conducting. The AFMs can be used to scan at atomic resolution all the material surfaces which may be either conducting or insulating.

2.7 Modes Of Operation Of AFM

The interaction between tip and sample depend on the separation between the two. Based upon this tip- sample interaction, there are three common modes of AFM.

(i) Contact mode

(ii) Tapping mode

(iii) Non-contact mode

The AFM can operate in a close contact mode in which the core- to-core repulsive forces with the surface dominate. In contact mode the AFM scans the sample surface with the cantilever tip remaining in its close contact and feeling throughout a repulsive force (see Figure 9).

In tapping mode the cantilever is allowed to oscillate at its resonant frequency (~100 KHz), as shown in Figure 10. The oscillating cantilever tip taps the specimen surface for a very short period of time. This method is usually employed for studying soft samples.

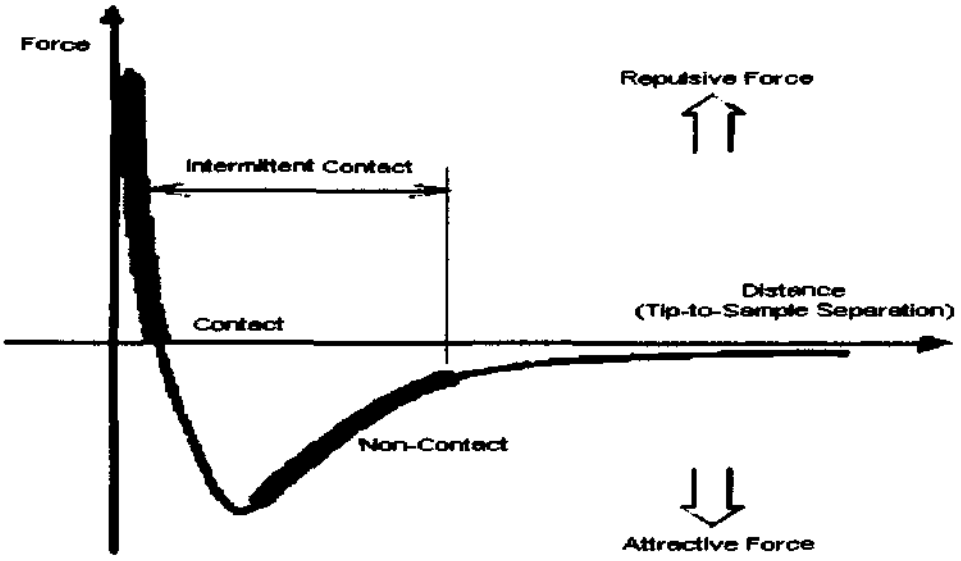

Figure 9. Inter-molecular force Curve.

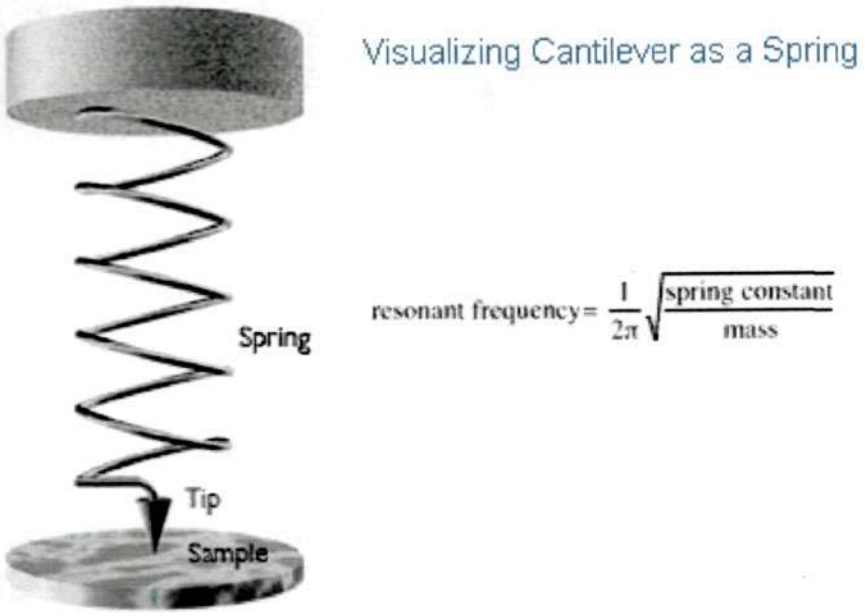

Figure 10. Visualization of cantilever as a spring.

In non-contact mode of AFM, the separation between the cantilever tip and the specimen surface is kept beyond the repulsive region of the inter-molecular force curve, as shown in Figure 9. In non- contact mode the relevant force is the gradient of the van – der Waals potential.

As in the STM case, a piezoelectric scanner is used. The vertical motions of the tip during the scanning may be monitored either by the interference pattern of a light beam from an optical fiber, as shown in Figure 11, or by the reflection of a laser beam, as shown in the enlarged view of the probe tip in the Figure 12.

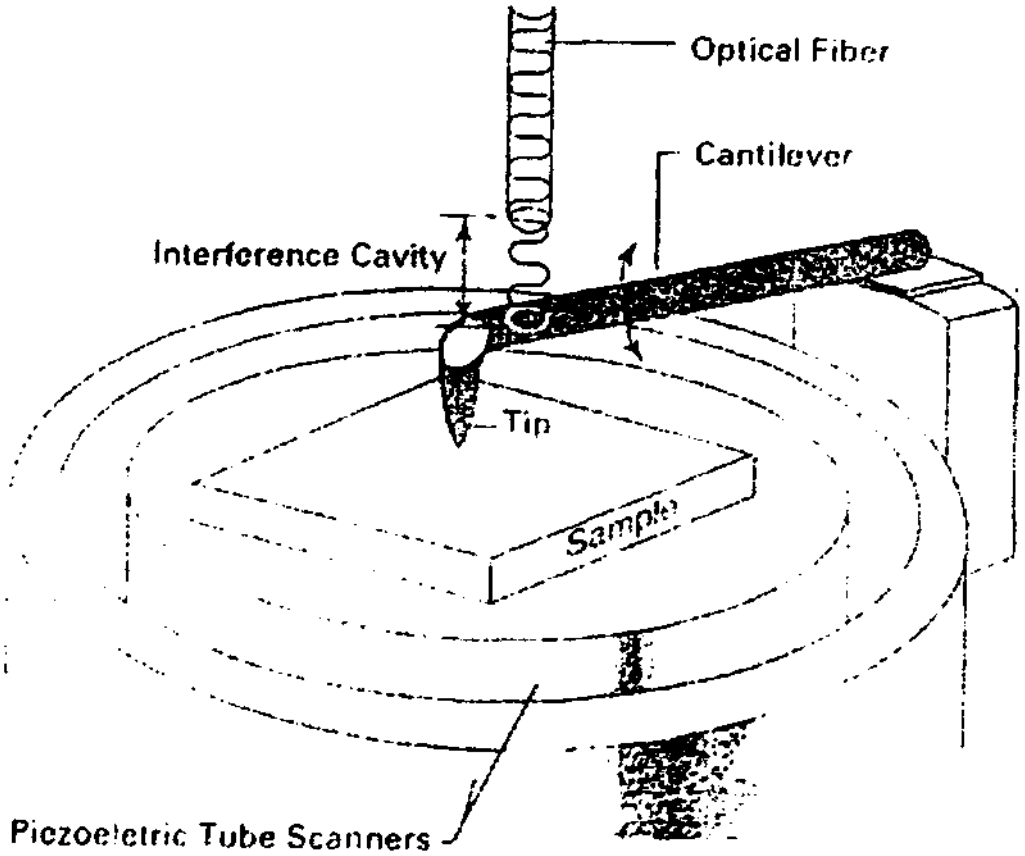

Figure 11. Sketch of an AFM showing the cantilever arm provided with a probe tip that traverse the sample surface through the action of the piezoelectric scanner. This Figure shows an interference deflection sensor.

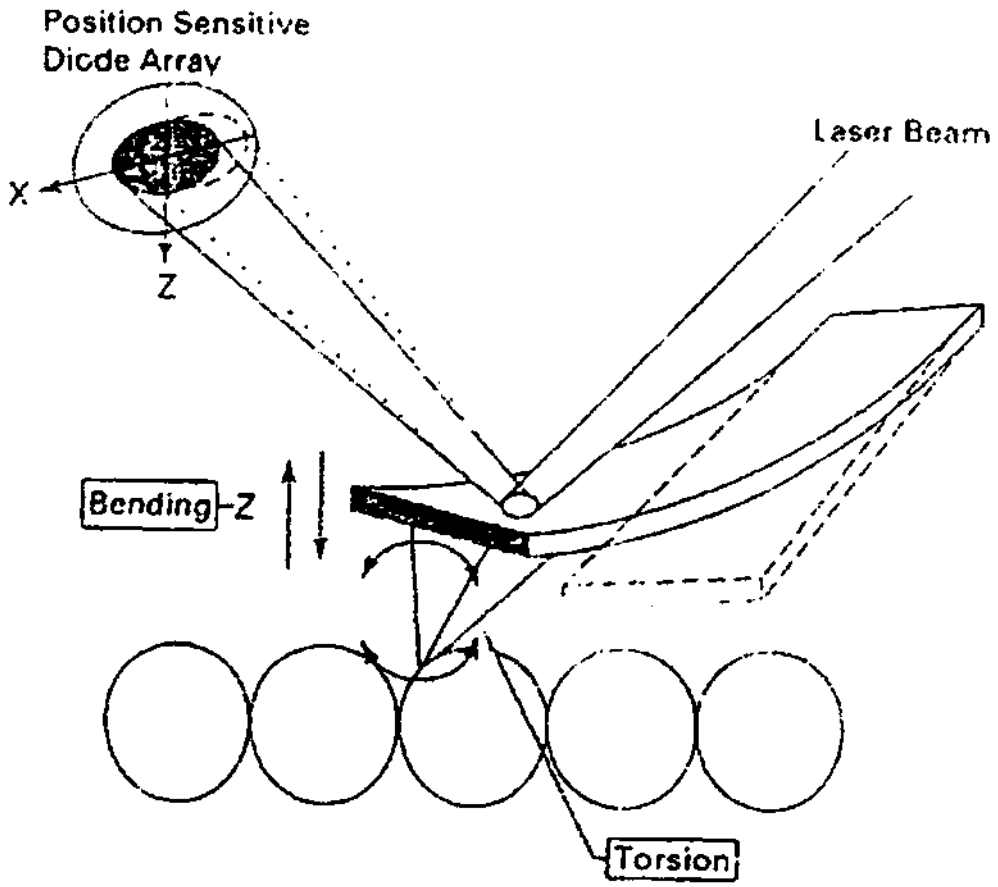

Figure 12. Shows an enlarged view of the cantilever and probe tip is provided with a laser beam deflection sensor. The sensors monitor the probe tip elevations upward from the surface during scan.

The AFM is sensitive to the vertical component of the surface forces. Binnig guessed that a cantilever with sharp tip may be bent by the forces between surface atoms and the cantilever tip. Knowing the force constant K of the cantilever and the magnitude of cantilever deflection Δx, the force between the tip and the surfaces can be calculated by Hooke's law:

$$F = K_{cantilever} (\Delta x)$$

The vertical deflection of the AFM cantilever is measured by an optical lever in which a laser beam is reflected off the cantilever onto a split photodiode whose different signal gives the magnitude of bending, as shown in Figure 13. The specimen or the tip may be moved in x-, y- and z- directions with the help of a suitable piezoelectric scanner. The scanner works on the well-known principle of piezoelectric effect in which an electric field applied across the faces of the piezoelectric material results in expansion in one direction and contraction in other direction.

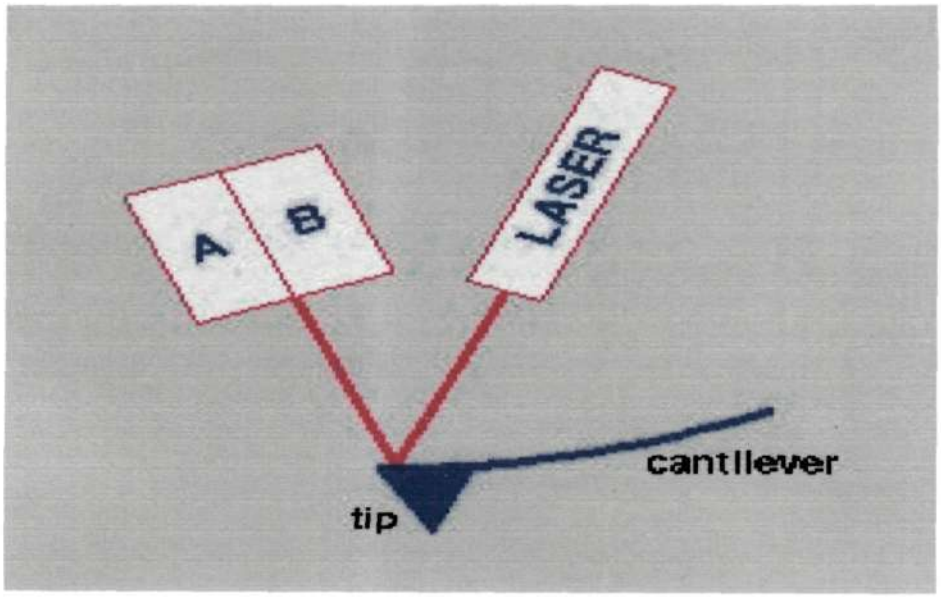

Figure 13. Shows bending of AFM cantilever.

A related but more versatile device called a friction force microscope (FFM), also sometimes referred to as a lateral force microscope (LFM), and simultaneously measures both normal and lateral forces of the surface on the tip.

The schematic diagram of AFM is shown in Figure 14.

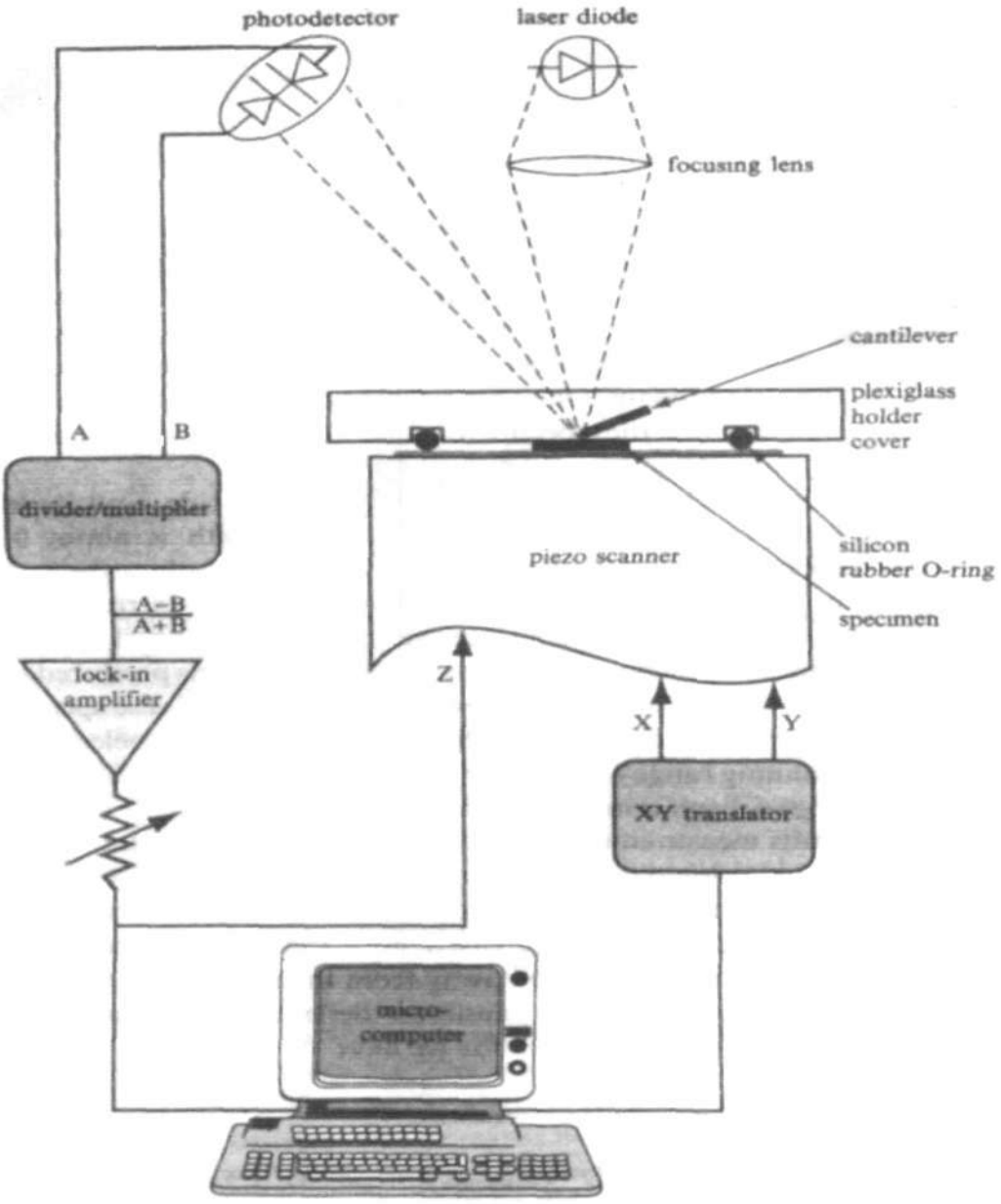

Figure 14. Schematic diagram of AFM.

Both, STM and AFM, can provide information on the topography and defect structure of a surface over distances close to the atomic scale. Figure 15 shows a three dimensional rendering of an AFM image of chromium deposited on a surface of SiO_2. The surface was prepared by the laser-focused deposition of atomic chromium in the presence of a gaussian standing wave that reproduced the observed regular array of peaks and valleys on the surface [11].

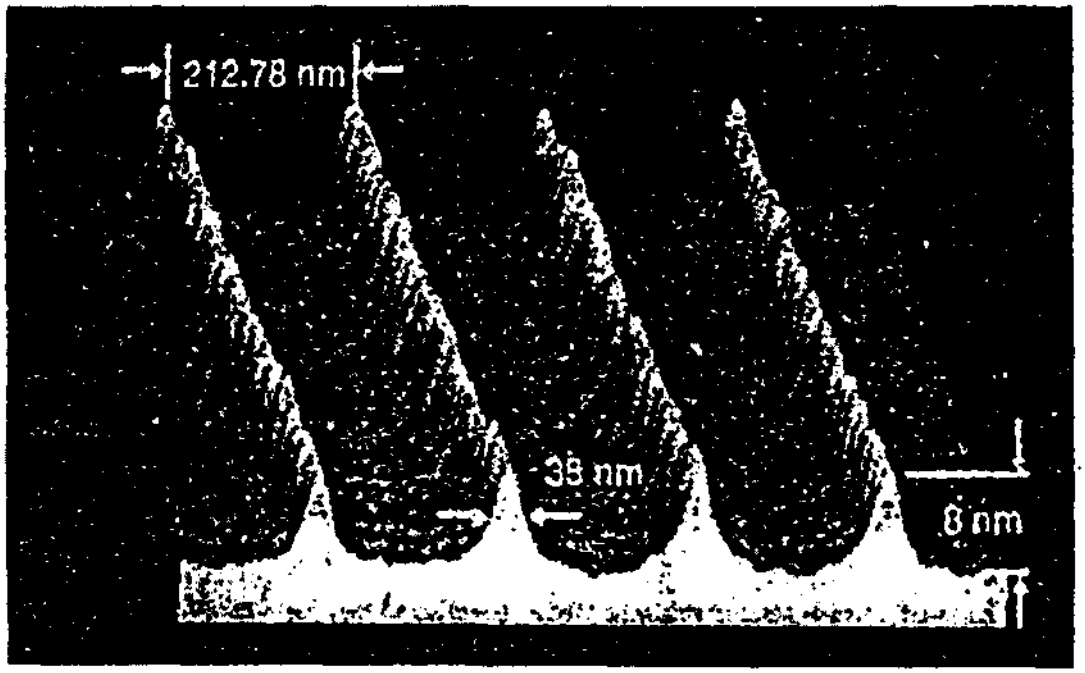

Figure 15. Three dimensional rendering of an AFM image of nanostructure formed by laser-focused deposition of atomic Cr in a gaussian standing wave on an SiO_2 surface.

2.8 AFM Probes

Since the resonant frequency of AFM cantilever has to be high they should have low spring constant as well as low mass. These parameters depend on the shape and size of the cantilever and the tip. For example, a rectangular cantilever of silicon with square pyramidal tip may have the following measurements:

Contact AFM Cantilever	**Tapping Mode Cantilever**
Length = 450 μm	Length = 125 μm
Width = 40 μm	Width = 30 μm
Thickness = 1-3 μm	Thickness =1-3 μm
Resonance Frequency = 6-20 KHz	Resonance Frequency = 6-20 KHz
Spring Constant = 0.22-0.66 N/m	Spring Constant = 0.22-0.66 N/m

Most commonly used materials for making AFM cantilevers are Si, Si_3N_4 and diamond. The parameters that determine the resonant frequency of a cantilever are shape, density and Young's modulus. Of these materials, silicon nitride (Si_3N_4) is a preferred material for the cantilevers because of its low cost and environmental friendliness especially with organic and biological samples. The common types of AFM tips are shown in Figure 16.

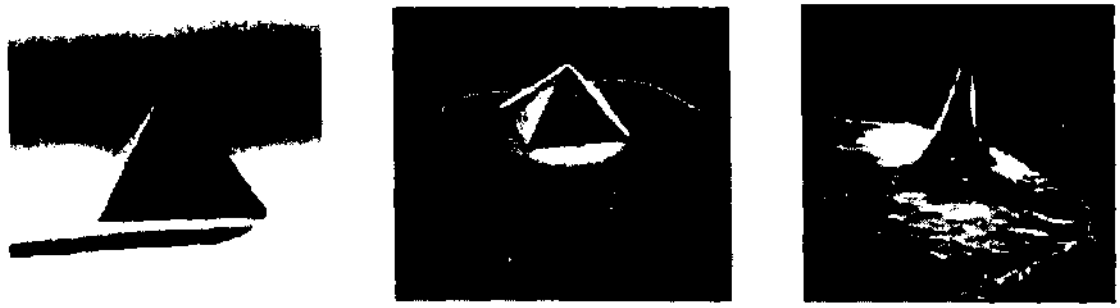

Figure 16. Common Types of AFM Tips (Jean-Paul Revel, Caltec)

2.9 SPMs Based On STMs And AFMs

Based on the principles of STMs and AFMs, two dozen scanning probe microscopes have been developed by measuring a local property of interest in each case for various scientific and industrial applications. For example the local property in such instruments may be orientation of magnetic domains with magnetic force microscope (MFM), differences in elastic modulii with a force modulation microscope (FMM), and difference in chemical forces across a surface in chemical force microscope (CFM). Some important SPMs are:

1. STM
2. AFM & LFM
3. SEFM-Scanning electrostatic force microscope
4. SFAM-scanning force acoustic microscope
5. SMM- scanning magnetic force microscope or MFM- magnetic force microscope
6. SNOM-scanning near field optical microscope
7. SThM- scanning thermal microscope

8. SEcM- scanning electrochemical microscope
9. SKPM-scanning Kelvin probe microscope
10. SCFM-scanning chemical force microscope
11. CFM –chemical force microscope
12. SICM-scanning Ion conductance microscope
13. SCM-scanning capacitance microscope
14. FMM-force modulation microscope

The Comparison of Conventional Microscopes with SPM is shown in Table 1.

Table 1. Comparison Of Conventional Microscopes With SPM

Comparison of Conventional Microscopes with SPM			
	Optical	**TEM**	**SPM**
Magnification	10^3	10^7	10^9
Price	$10,000	$250,000	$100,000
Technology Age	200 years	50-70 years	20 years

References

1. Feynman R.P.: "There is Plenty of Room at the Bottom", APS Meeting, California Institute of Technology, December 26, 1959.
2. Kroto, H.W. and Smalley, R.E., (1985) Nature, 318, 162-163.
3. Binnig, G. and Rohrer, H. (1982) Helv. Phys. Acta. 55, 726-735
4. Iijima, S., (1991) Nature 354, 56.
5. Binnig, G., Quate, C.F., and Gerber, Ch., (1986) Phys. Rev. Lett. 56, 930-933.
6. Bayburt, T., Carlson, J., Godfrey, B., M.Shank-Retzlaff, and sliger, S. G. in Nalwa (2000), Vol.5, chapter 12, p.641.
7. Giaever, I., (1960), Phys. Rev. Lett. 5, 147-148.
8. Stroscio, J.A., Eigler, D.M. (1991) Science 254, 1319.
9. Crommie, M.F., Lutz, C.P., and Eigler, D.M. (1994) Nature 369, 464.
10. Yang, J., Tamm, L. K., Somlyo, A. P. and Shao, Z., Journal of Microscopy 171, 183-198, 1993.
11. J. J. McClelland, Gupta, R., Jabbour, J. Z., and Celotta, R. L., Aust J. Phys. 49, 555 (1996).

Chapter 3

Fullerenes And Carbon Nanotubes

Chapter 3

Fullerenes And Carbon Nanotubes

In this chapter we review carbon materials from the standpoint of nanotechnology. The unusual features of carbon materials stem from the ability of carbon to form materials with vastly different structures and hence with vastly different properties. The major focus of this chapter is on the ability of carbon to form zero dimensional quantum dots of sub nanometer dimensions in the form of fullerenes, and one-dimensional quantum wires in the form of carbon nanotubes. Graphite is the ground state for a system containing a huge number of carbon atoms; there is a large energy per carbon atom associated with the edge sites for a small graphene sheet (defined as a single isolated layer of the graphite lattice). Thus, to avoid the occurrence of edge sites, small numbers of carbon atoms form closed shell configurations such as fullerenes and carbon nanotubes [see Figure 1]. The structure and properties of fullerenes and carbon nanotubes are reviewed in this chapter in the context of nanotechnology.

A. Fullerenes

3.1 Fullerenes (C_{60}) As Nanostructures

Fullerene solids differ from conventional electronic materials because, in common with most polymeric materials, the fullerene molecule is the fundamental building block of crystalline phase. Unique features about fullerenes include the structural perfection and reproducibility of these sub nanometer building blocks.

In the preparation of fullerenes by any of the conventional synthesis methods (by carbon arc discharge, laser pyrolysis or combustion flames) the fullerene species of greatest abundance by far is C_{60}, the most stable of the fullerenes and the fullerene with the greatest symmetry [1]. Every C_{60} molecule is identical, except for the possible presence of the ^{13}C isotope, with a 1.1% natural abundance, which can substitute randomly for ^{12}C in the caged molecule. C_{60} molecules thus form a very small (0.71 nm diameter) monodisperse nanostructure of high (icosahedral I_h) symmetry. Since all C_{60} fullerene molecules (0.7 nm diameter) are identical to one other, they perhaps represent the most reproducible currently available nanostructure. The C_{60} is already attractive for use as a monodisperse, reproducible, self assembled nanostructure. Present trends of rapidly decreasing costs and increasing purity through better and cheaper fabrication technology are making C_{60} even more attractive relative to other nanostructures for specific applications. An attractive feature of fullerenes is their ready accessibility to doping, charge transfer, and the resulting control of the electronic properties of the nanostructures. As a result of their unique structures and properties, potential applications for fullerene based electronic materials are suggested. Because of the simplicity of C_{60}

relative to other fullerenes and its relatively high abundance, most of the discussion of fullerenes in this review is for C_{60}.

3.2 Structure Of C_{60}

The C_{60} molecule has been named fullerene after the architect and inventor R. Buckminster Fuller who designed the geodesic dome that resembles the structure C_{60} [2]. Originally the molecule was called *buckminsterfullerene*, but this name is a bit unwieldy, so it has been shortened to *fullerene*. A sketch of the C_{60} fullerene molecule shown in Figure (1a).

To a good approximation, the 60 carbon atoms in C_{60} are located at the vertices of a regular truncated icosahedron. The average nearest neighbor carbon-carbon (C-C) distance a_{c-c} in C_{60} is very small (~0.144nm) and is almost identical to that in graphite (0.142 nm). Each carbon atom in C_{60} (and also in graphite) is trigonally bonded to three other carbon atoms and 20 of the 32 faces on the regular truncated icosahedron are hexagons, the remaining 12 beings pentagons. Thus, we may consider the C_{60} molecule as a " rolled-up" graphene sheet (a single layer of crystalline graphite) which forms a closed shell, in keeping with Euler's theorem, which states that a closed surface consisting of hexagons and pentagons has exactly 12 pentagons and an arbitrary number of hexagons [3].

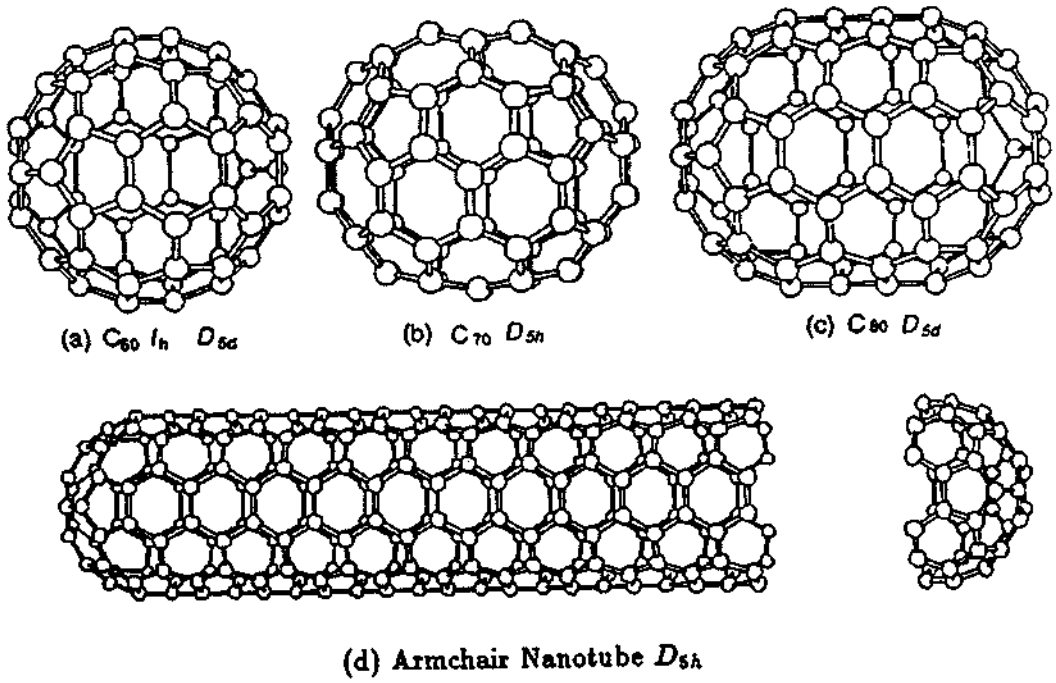

Figure 1. (a) C_{60}, (b) C_{70}, (c) C_{80}, (d) A carbon nanotube. Here D_{5D} is a subgroup of the icosahedral group I_h, exhibiting inversion symmetry.

The introduction of pentagons gives rise to curvature in forming a closed surface. To minimize local curvature the pentagons become separated from each other in the self-assembly process, giving rise to the isolated pentagon rule, an important rule for stabilizing C_{60} clusters. The high reproducibility of C_{60} in the self-assembly process relates to the fact that the smallest cluster to obey the isolated pentagon rule is C_{60} and that there is only one way to assemble 60 carbon atoms in a closed cage configuration which obeys the isolated pentagon rule. The structure is shown in Figure (1a). The diameter of C_{60} molecule is 0.710 nm, treating the carbon atoms as points [4,5,6].

From Euler's theorem it follows that the smallest possible fullerene is C_{20} which would form a regular dodecahedron with 12 pentagonal faces [7], but this structure is

energetically unfavorable in accordance with isolated pentagon rule, because of its high local curvature and high strain. Since the addition of a single hexagon adds two carbon atoms, all fullerenes Cn_c must have an even number of carbon atoms n_c, in agreement with the observed mass spectra for fullerenes [8]. An estimate for the diameter of a fullerene can be obtained from the relation for an icosahedral fullerene

$$d_i = a_{c-c}\sqrt{\frac{15n_c}{2\pi}}$$

Where a_{c-c} =0.144 nm is the average nearest neighbor carbon- carbon distance. Each fullerene Cn_c can thus be considered as a nanostructure with diameters less than 3 nm for $n_c < 10^3$. Although each carbon atom in C_{60} is equivalent to every other carbon atom, the three bonds emanating from each atom are not equivalent [see Figure 1(a)]. Each of the four valance electrons of each carbon atom is engaged in covalent bonds, so that two of the three bonds on the pentagon perimeter are electron- poor single bonds, and one between two hexagons is an electron- rich double bond. Since each carbon atom has its valance requirements fully satisfied, a solid composed of C_{60} molecules is expected to form a Van der waals- bonded crystal which is noncoducting (an insulator or a semiconductor).

3.3 Alkali-Doped C_{60}

It has been found [9] that the intercalation of alkali metals into C_{60} to a stoichiometry M_3C_{60} (where M = K, Rb, Cs) greatly modifies the electronic properties of the host fullerenes and yields a conducting material with a relatively high superconducting transition temperature [10]. In the intercalation process, the guest

species is introduced into the interstitial positions between adjacent molecules (exohedral locations).

In fact a soccer ball has the same geometric configuration as fullerene. These ball like molecules bind with each other in the solid state to form a crystal lattice having a face centered cubic structure shown in Figure 2. In the lattice each C_{60} molecule is separated from its nearest neighbor by 1 nm (the distance between their centers is 1 nm), and week forces called Van der waals forces hold them together. In the face centered cubic fullerene structure, 26 % of the volume of the unit cell is empty, so alkali atoms can easily fit into the

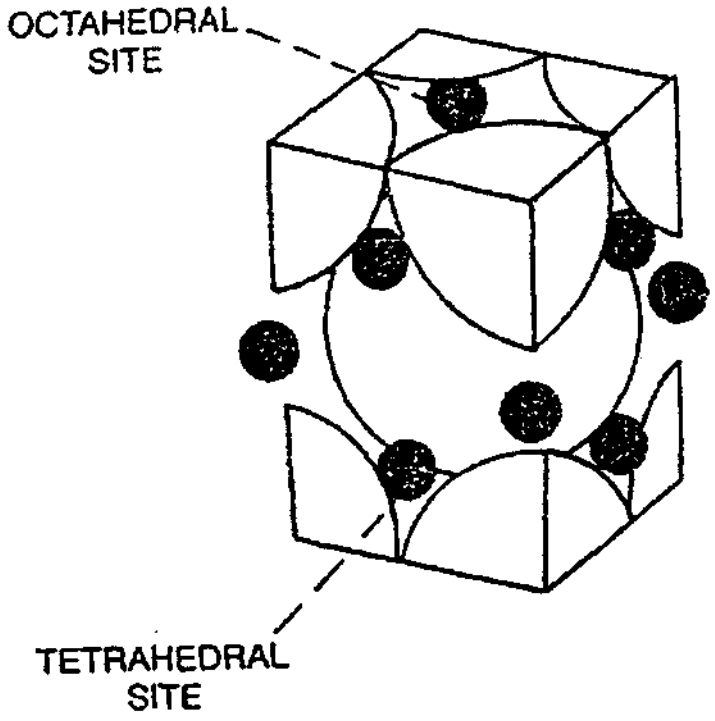

Figure 2. Crystal lattice unit cell of C_{60} molecules (large spheres) doped with alkali atoms (dark circles).

empty spaces between the molecular balls of the material. When C_{60} crystals and alkali metal (such as potassium metal) are placed in evacuated tubes and heated to 400° C, potassium vapor diffuses into these empty spaces to form the compound K_3C_{60}. Thus, the C_{60} crystal is an insulator, but when doped with an alkali atom it becomes electrically conducting. Figure 2 shows the location of the alkali atoms in the lattice where they occupy the two vacant tetrahedral sites and a larger octahedral site per C_{60} molecule. In the tetrahedral site the alkali atom has four surrounding C_{60} balls, and in the octahedral site there are six surrounding C_{60} molecules. When C_{60} is doped with potassium to form K_3C_{60}, the potassium atoms become ionized to form K^+ and their electrons become associated with the C_{60}, which becomes a C_{60}^{3-} triply negative ion. Thus each C_{60} has three extra electrons that are loosely bonded to the C_{60}, and can move through the lattice making C_{60} electrically conducting. In this case the C_{60} is said to be electron-doped. Charge transfer can take place between the M atoms (where M = K, Rb, Cs) and the fullerene molecules, so that the M atoms become positively charged ion and the molecules become negatively charged anions with predominately-delocalized electrons.

With exohedral doping, the conductivity of fullerene solids can be increased by many orders of magnitude [11]. Among the alkali metals, Li, Na, K, Rb, and Cs and their alloys have been used as exohedral dopants for C_{60} [12,13]. The doping of the C_{60} with alkali metals can be achieved in a two-temperature oven, similar to the apparatus used to prepare alkali-metal graphite intercalation compounds [11,14]. Doping fullerenes with acceptors has been more difficult than with donors because of the high electron affinity of C_{60} (see table1 and 2)[1]. Although a very few stable compounds with acceptor- type dopants have been synthesized [15,16], acceptor doping has not been important for the synthesis of electronic materials based on fullerenes.

Table 1. Physical Constants For Crystalline C_{60}

S.No.	Quantity	Value
1	Fcc lattice constant	1.417 nm
2	C_{60}-C_{60} distance	1.002 nm
3	Work function	4.7 ± 0.1 eV
4	Thermal conductivity (300K)	0.4 W/mk
5	Electrical conductivity (300K)	1.7×10^{-7} S/cm
6	Melting temperature	1180^{0}C

Table 2. Physical Constants For C_{60} Fullerene Molecules

S.No.	Quantity	Value
1	Average C-C distance	0.144 nm
2	C-C bond length on a pentagon	0.146 nm
3	C-C bond length on a hexagon	0.140 nm
4	C_{60} mean molecular diameter	0.710 nm
5	Moment of inertia I	1.0×10^{-43} kg m^2
6	Volume per C_{60}	$1.87 \times 10^{22}/cm^3$
7	Number of distinct C-C bonds	2
8	Binding energy per atom	7.40 eV
9	Electron affinity	2.65 ± 0.05 eV
10	Ionization potential	7.58 eV

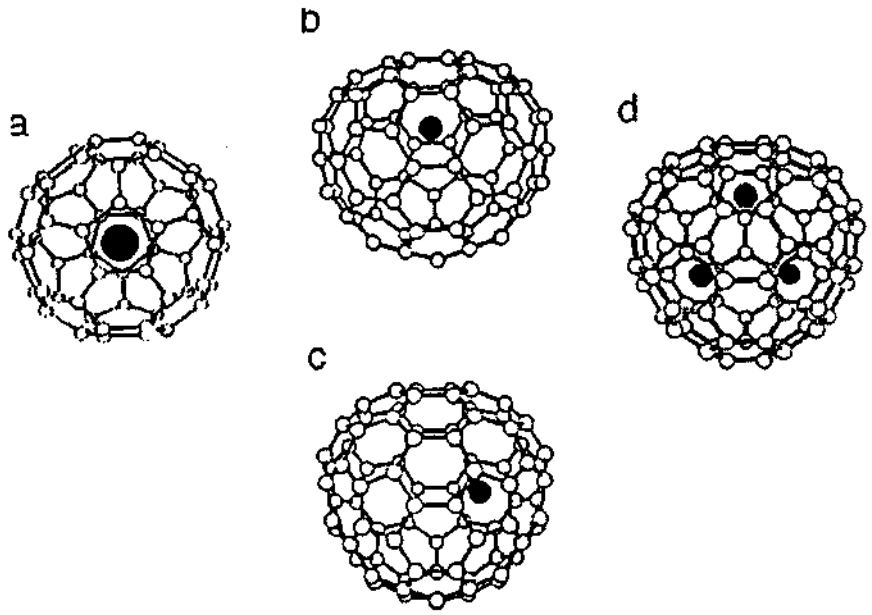

Figure 3. Structural models for various endofullerenes. (a) With M atom at the center of the C_{60}. (b, c) With the M atoms at two different off-center positions in C_{60}. (d) With three M atoms at different postions in C_{60}.

Regarding metallofullerenes, many guest species can be inserted into the interior hollow core of the C_{60} molecule to form an endohedrally doped molecular unit, and the insertion of one, two, or three metal species inside a single fullerene cage is common [17]. The endohedral fullerene configuration has, for example, been denoted by $La@C_{60}$ for one endohedral lanthanum in C_{60}, or, $Y_2@C_{82}$ for two Y atoms inside a C_{82} fullerene. [see Figure 3].

3.4 Superconductivity In C_{60}

Superconductivity is a state of matter in which the resistance of a sample becomes zero, and in which no magnetic field is allowed to penetrate the sample. The latter manifests itself as a reduction of the magnetic susceptibility χ of the sample to $\chi = -1$ (in

the MKS system). The first reported superconductor in the fullerene family was K_3C_{60} with $T_c \sim 19$ K [10], and subsequent work has revealed superconductivity with $T_c \sim 40$ K in Cs_3C_{60} under a pressure of 12 kbar [18]. Figure 4 shows the drop in magnetization indicative of the presence of superconductivity [19].

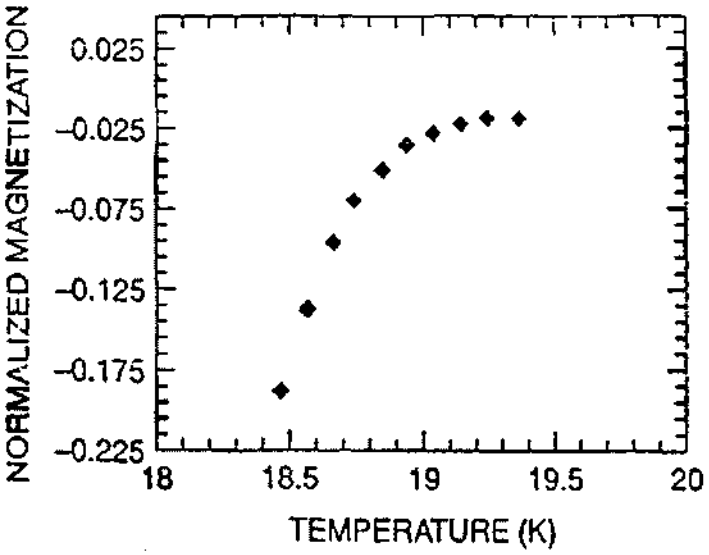

Figure 4. Magnetization versus temperature for K_3C_{60} showing the transition to the superconducting state.

It was found that many alkali atoms could be doped into the lattice, and the transition temperature increased to as high as 33 K in Cs_2RbC_{60}. As the radius of the dopant alkali atom increases, the cubic C_{60} lattice expands, and the superconducting transition temperature goes up. Figure 5 is a plot of the transition temperature versus the lattice parameter [19].

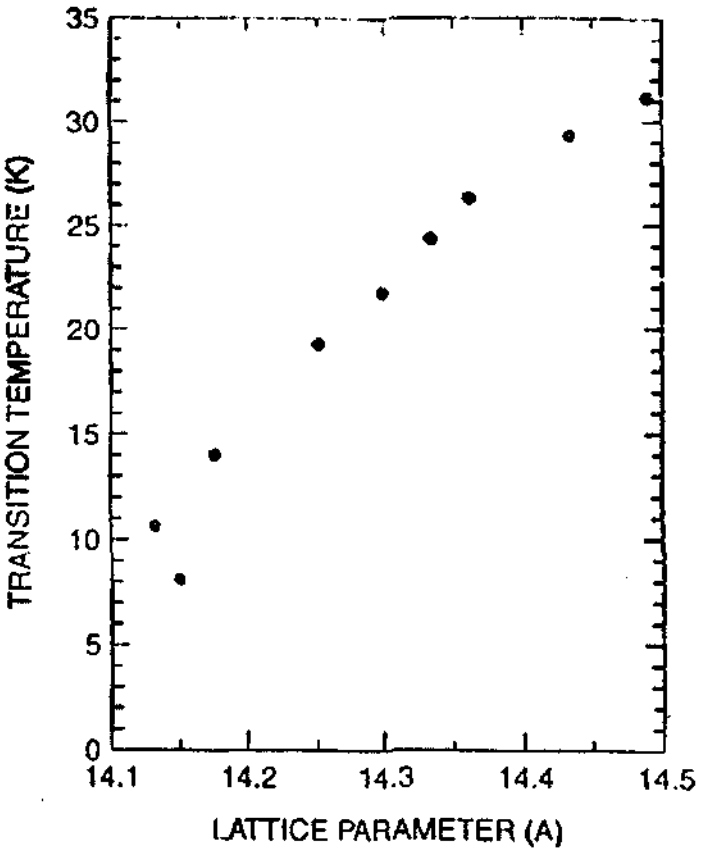

Figure 5. Transition temperature of A_3C_{60} versus lattice parameter, where A is an alkali atom. (10 A° = 1nm).

The discovery of superconductivity in these compounds further spurred research activity in the field of C_{60} related materials.

3.5 Synthesis Of Fullerenes

Synthesis methods for fullerenes are rapidly improving, thereby increasing yields and lowering costs. Likewise, separation and purification methods are also improving rapidly making available C_{60} samples with purities well beyond 99 %. Through the use of

scanning tunneling microscopy (STM), physical measurements on periodic arrays of higher mass fullerenes and metallofullerenes can be made.

Fullerenes are usually synthesized using an arc discharge between graphite electrodes (20V, 60A) in approximately 200 torr of He gas. The heat generated at the contact point between the electrodes evaporates carbon to form soot and fullerenes, which condense on the water-cooled walls of the reactor. This discharge produces a carbon soot which contains up to ~15 % fullerenes: C_{60} (~13 %) and C_{70} (~2 %). The fullerenes are next separated from the soot according to their mass (which is proportional to the number of carbon atoms in the fullerene molecule) using liquid chromatography and a solvent such as toluene for the chromatography column. Extraction and purification steps follow the separation to yield powder samples of specific fullerenes.

Metallofullerenes are prepared by endohedral doping of guest species such as alkali metal ions into the interior of the fullerene molecule. The synthesis is carried out by impregnating the positive electrode with graphite powder mixed with the desired dopants. During the arc discharge process, the dopant species are released into the plasma gas and becomes entrained within the fullerenes. Sophisticated liquid chromatography techniques are used for concentrating the minute amounts of a given metallofullerene that are prepared in the synthesis process, which is followed by further separation and purification steps [20]. Thus far, only small quantities of endohedrally-doped fullerenes have been prepared and only limited investigations of the physical properties of endohedrally-doped materials have been reported [20]. Property measurements of fullerenes are made either on powder samples, films or single crystals. C_{60} powder is obtained by vacuum evaporation of the solvent from the solution. Single crystals and polycrystalline films are then prepared from these purified powders. Fullerene films are prepared by vacuum sublimation of the fullerenes on substrate selected for the specific use of the films.

3.6 Crystalline C_{60}

In the crystalline phase, the C_{60} molecules have cubic structure with a lattice constant of 1.417 nm, a nearest neighbor C_{60} – C_{60} distance of 1.002 nm [21] and a density of 1.72 g/cm^3. At room temperature, the molecules rotate rapidly with full rotational freedom, and the centers of the molecules are arranged on a face centered cubic (fcc) lattice with one C_{60} molecule per primitive fcc unit cell [see figure 6(a)], or 4 molecules per simple cubic unit cell [see figure 6(b)].

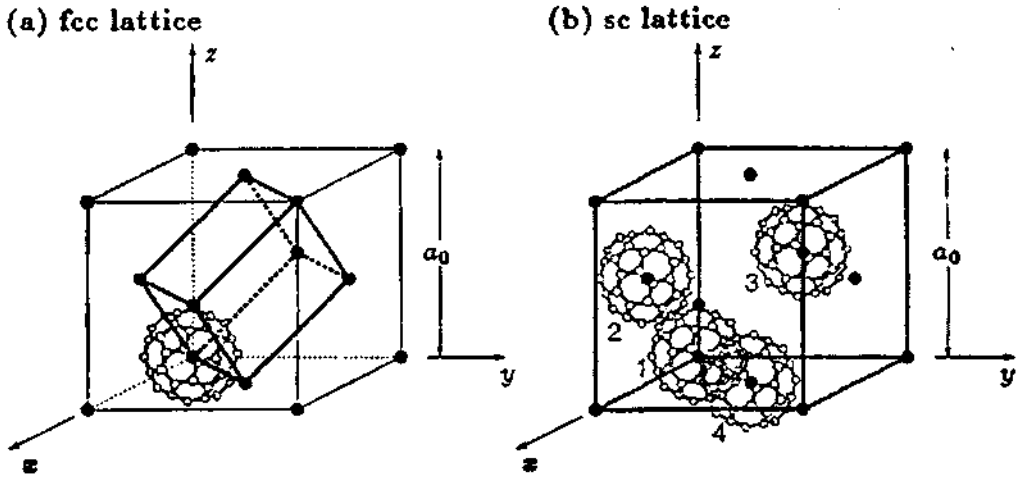

Figure 6. Crystal structures for (a) the high temperature fcc phase of C_{60} and (b) the low temperature sc phase of C_{60}.

3.7 Applications Of Fullerenes

Since all C_{60} molecules are identical and since C_{60} can be synthesized to high purity and in large quantities (gram quantities) at relatively low cost, the C_{60} molecule is attractive for a variety of nanostructure applications. Since C_{60} molecules strongly bonded internally, chemically inert, nearly spherical, and nonpolar due to symmetry, and

considered to be nanostructures of nanometer size which can be manipulated using STM probe tips, just as is done for noble gas atoms. Moreover, some other manipulation may be possible for C_{60} that are not possible for any other species. For instance, it has been proposed, that a C_{60} molecule can be "rolled" (diffused) along a suitable ionic substrate by a rotating external electric field, utilizing the large size and polarizability of C_{60} as shown in Figure 7.

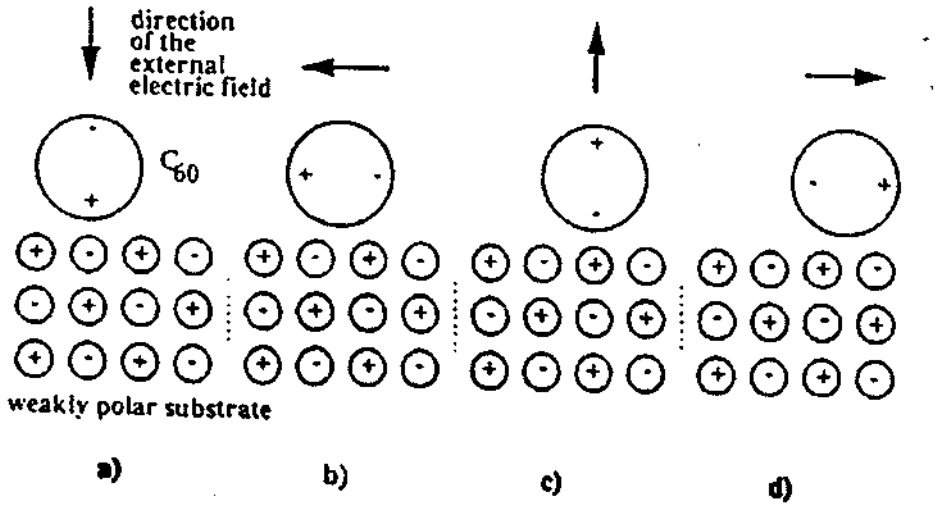

Figure 7. Shows the principle of moving C_{60} molecules by a rotating external electric field. The successive directions of the field are shown in (a) through (d).

It has been proposed that nanocrystalline C_{60} islands grown on certain types of substrate could be used as transport devices for fabrication process of nanometer sized machines. Fullerene based nanodevices may be capable of biological interfacing. Fullerenes could also be used to enhance the resolution of STM tips, utilizing the uniform structure of the C_{60} molecules.

B. Carbon Nanotubes

3.8 Carbon Nanotubes As Nanostructures

In addition to quantum dot 0D fullerene nanostructures, there is a possibility to synthesize cylindrical tube of graphene sheet (carbon nanotube), which can be classified as 1D quantum wires. The field of carbon nanotubes research was greatly stimulated by the initial report of the experimental observation of carbon nanotubes [22] and the subsequent report of conditions for the synthesis of large quantities of nanotubes [23,24]. Various experiments carried out thus far (high resolution TEM, STM, resistivity, Raman scattering and susceptibility) are consistent with identifying the carbon nanotubes with rolled up cylinders of graphene sheets of sp^2 bonded carbon atoms. They can be prepared both as monolayer, called single wall nanotubes (SWNTs) and multilayer nested concentric, called multi wall nanotubes (MWNTs). The earliest observations of carbon nanotubes with very small (nanometer) diameter [22] were based on high-resolution transmission electron microscopy (TEM) measurements, providing evidence for micrometer long tubes, with cross sections showing several concentric coaxial tubes and a hallow core. In Figure 8, the observations of multilayer concentric carbon nanotubes are shown. Here we see only multi-layer carbon nanotubes, but one tube has only two coaxial carbon cylinders as shown in Figure 9.

A single-wall nanotube is defined by a cylindrical graphene sheet with a diameter of about 0.7-10.0 nm, though most of the observed SWNTs have diameters < 2 nm. If we neglect the two ends of a carbon nanotube and focus on the large aspect ratio of cylinder (ie. Length/diameter, which can be as large as 10^4-10^5), these nanotubes can be considered as one- dimensional nanostructures

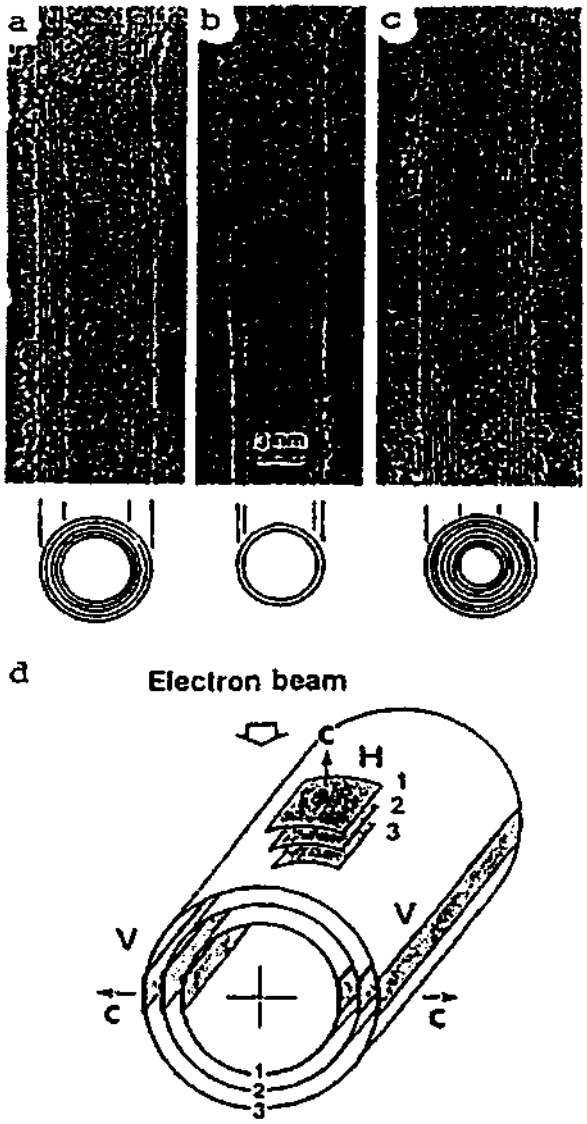

Figure 8. The observation of N concentric carbon nanotubes with various inner diameters. (a) N = 5, (b) N = 2, (c) N = 7. Each cylinder is described by its diameter and chiral angle The sketch (d) indicates how interference pattern for the parllel planes are used to determine the chiral angle θ, which is the angle between the tube axis and the nearest zigzag axis defined in Figure 10(a).

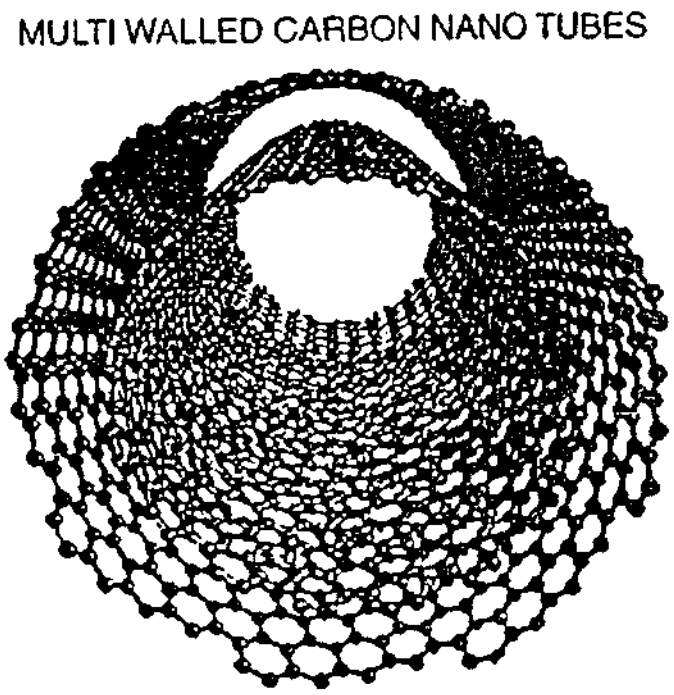

Figure 9. Illustration of a nested nanotube in which one tube is inside the another.

3.9 Structure Of Carbon Nanotube

The structure of carbon nanotubes has been explored by high resolution TEM and STM, yielding direct confirmation that the nanotubes are cylinders derived from the honeycomb lattice (graphene sheet). Although carbon nanotubes are not actually made by rolling graphene sheets, they can be described as graphene sheets rolled into a cylindrical shape so that the structure is one-dimensional with axial symmetry, and in general exhibiting a spiral conformation, called chirality. The chirality is given by a single vector called the chiral vector. The chirality of a carbon nanotube is conveniently explained in terms of 1D unit cell as shown in Figure 10(a).

The circumference of any carbon nanotube is expressed in terms of the chiral vector, which is given by

$$\vec{C}_h = n\hat{a}_1 + m\hat{a}_2 \equiv (n,m), \qquad \text{(n, m are integers, } 0 \leq |\,m\,| \leq n)$$

Where $\hat{a}_1$ and $\hat{a}_2$ are unit vectors. The chiral vector connects two crystallographically equivalent sites on a 2D graphene sheet [see Figure 10 (a)] [25]. The construction in Figure 10 shows the chiral angle θ between $\vec{C}_h$ and the zigzag direction ($\theta = 0^0$) and unit vectors $\hat{a}_1$ and $\hat{a}_2$ of hexagonal honeycomb lattice. An ensemble of chiral vectors specified by pairs of integers (n, m) denoting the chiral vector $\vec{C}_h$ is given in Figure 10(b), in which the encircled dots denote metallic behavior of tubes while small dots are for semiconducting tubes [26]. In Figure 10(a), the unrolled honeycomb lattice of nanotube is shown, in which $\overline{OB}$ is the direction of the nanotube axis, and the direction of $\overline{OA}$ corresponds to the equator. The vectors $\overline{OA}$ and $\overline{OB}$ define the chiral vector $\vec{C}_h$ and the 1D translation vector $\vec{T}$ of a carbon nanotube respectively. The translation vector $\vec{T}$ is defined to be the unit vector of 1D carbon nanotube. The vector $\vec{T}$ is parllel to the nanotube axis and is normal to the chiral vector $\vec{C}_h$ in the honeycomb lattice in Figure 10(a). The lattice vector $\vec{T}$ shown as $\overline{OB}$ in the Figure 10(a) can be expressed in terms of basis vectors $\hat{a}_1$ and $\hat{a}_2$ as:

$$\vec{T} = t_1\hat{a}_1 + t_2\hat{a}_2 \equiv (t_1,t_2),$$

where t_1 and t_2 are integers. The translation vector $\vec{T}$ corresponds to the first lattice point of 2D graphene sheet through which vector $\overline{OB}$ (normal to the chiral vector $\vec{C}_h$) passes.

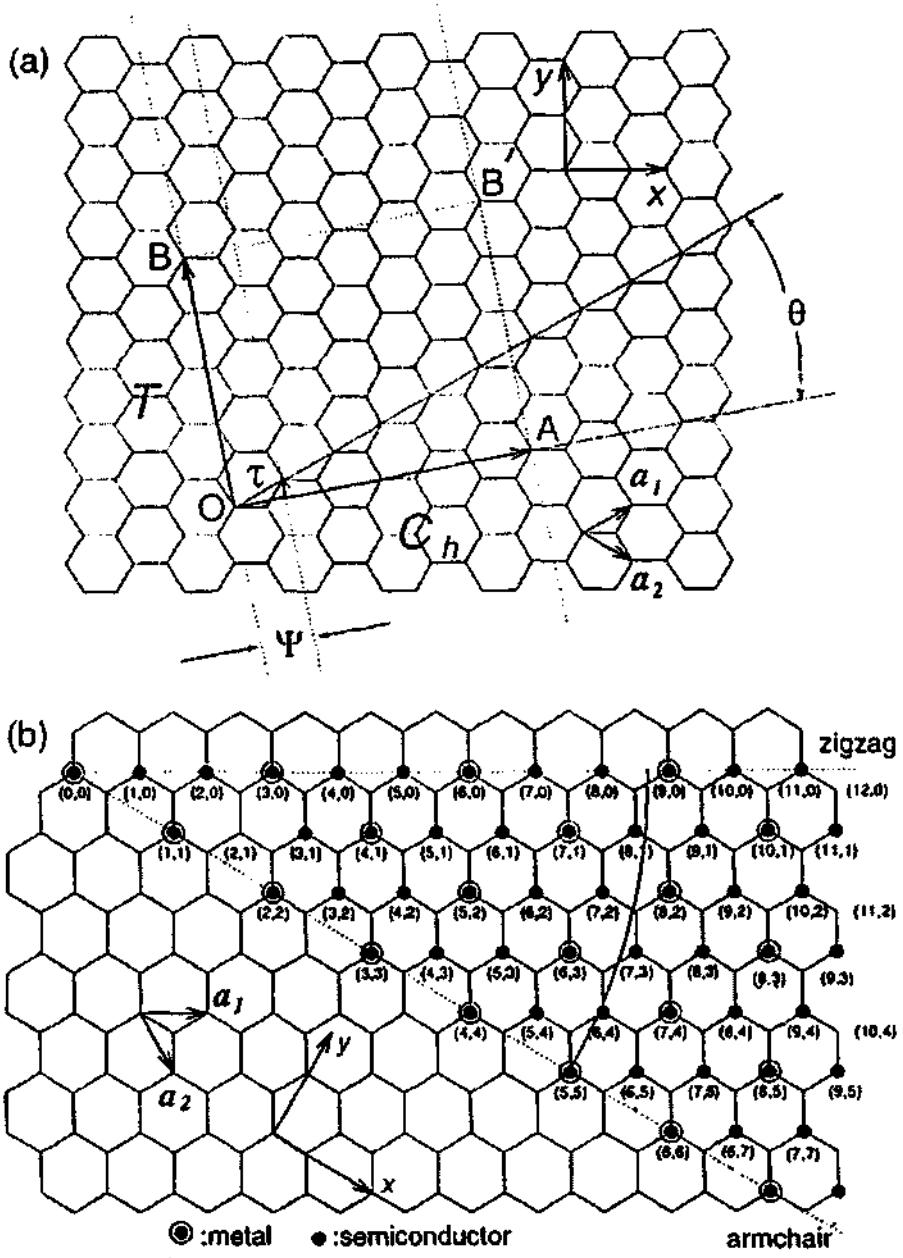

Figure 10. (a) The Chiral vector $\overline{OA}$ or $\vec{C}_h$ is defined on the honeycomb lattice of carbon atoms by unit vectors $\hat{a}_1$ and $\hat{a}_2$ and the chiral angle θ with respect to the zigzag axis. Along the zigzag axis θ = 0°. Also the translation vector $\overline{OB} = \vec{T}$ is shown along tube axis. (b) Possible vectors specified by the pairs of integers (n, m) for general carbon nanotubes, including zigzag, armchair, and chiral tubes. The encircled dots denote metallic while the small dots are for semiconducting tubes.

3.10 Classification Of Carbon Nanotubes

An interesting and essential fact about the structure of a carbon nanotube is the orientation of the six-membered carbon ring (hereafter called a hexagon) in the honeycomb lattice relative to the axis of the nanotube [27]. Three examples of single wall carbon nanotubes (SWCNTs) are shown in Figure 11.

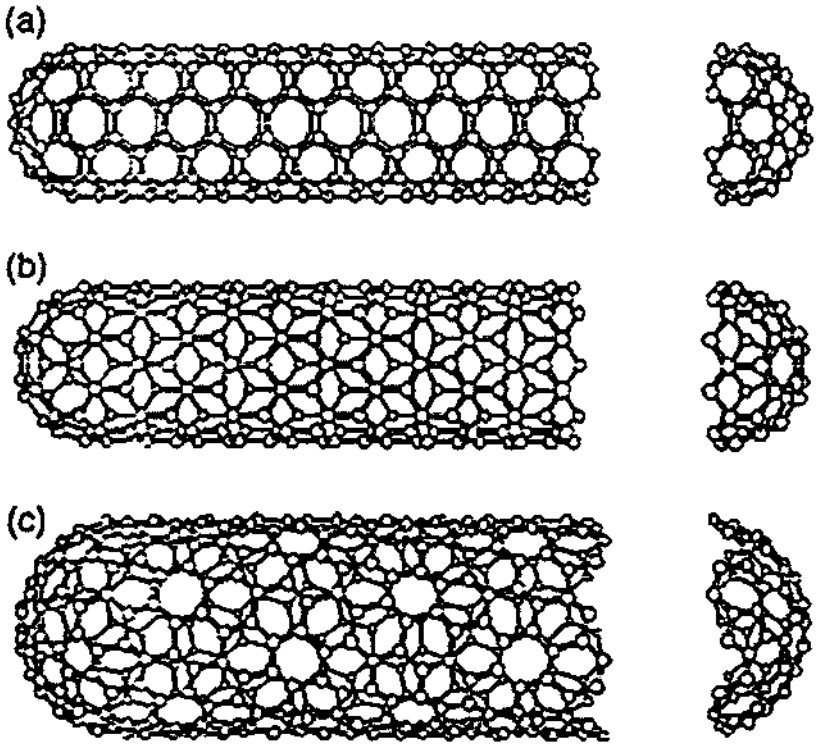

Figure11. Classification of carbon nanotubes: (a) armchair, (b) zigzag, and (c) chiral nanotube.

From the Figure 11, it can be seen that the direction of the six-membered ring in the honeycomb lattice can be taken almost arbitrarily, without any distortion of the hexagons except for the distortion due to the curvature of the carbon nanotube. This fact provides many possible structures for carbon nanotubes, even though the basic shape of

carbon nanotube wall is cylinder. The termination of each of the three nanotubes are shown in Figure 11. The terminations are often called caps or end caps and consist of a "hemisphere" of a fullerene. Each cap contains six pentagons an appropriate number and placement of hexagons that are selected to fit perfectly to the long cylindrical section. The cylinder connecting the two hemispherical caps is formed by superimposing the two ends of the vector $\vec{C}_h$ and the cylinder joint is made along the two lines OB and AB' in Figure 10(a). These two lines are perpendicular to the vector $\vec{C}_h$ at each end [25]. The chiral tube, thus generated has no distortion of bond angles other than distortions caused by the cylindrical curvature of the tube. Differences in chiral angle θ and in the tube diameter give rise to differences in the properties of the various tubes. With the help of Figure 10(b), the carbon nanotubes can be classified in terms of chiral angle θ and (n, m) integers for chiral vector $\vec{C}_h$. In (n, m) notation for vector $\vec{C}_h$, the vectors (n, 0) or (0, m) denote zigzag nanotube (chiral angle $\theta = 0^0$) and the vectors (n, n) denote armchair nanotube (the armchair tube corresponds to chiral angle of $\theta = 30^0$). All other vectors (n, m) correspond to chiral nanotubes. A classification of carbon nanotubes in terms of chiral angle θ and integer (n, m) is given in table 3.

Table 3. Classification Of Carbon Nanotubes

S. No.	Type of Nanotube	Chiral angle θ	C_h	Shape of cross- section
1	Zigzag	0^0	(n, 0)	Trans type 
2	Armchair	30^0	(n, n)	Cis type 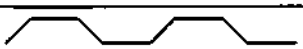
3	Chiral	$0^0 < \theta < 30^0$	(n, m)	Mixture of cis and trans.

3.11 Mathematical Analysis

(i) To find out tube diameter (d_t)

We know that the chiral vector $\vec{C}_h$ (along $\overrightarrow{OA}$) in Figure 10 (a) is defined as:

$$\vec{C}_h = n\hat{a}_1 + m\hat{a}_2 \tag{1}$$

and the translation vector $\vec{T}$ (along $\overrightarrow{OB}$) is defined as:

$$\vec{T} = t_1\hat{a}_1 + t_2\hat{a}_2 \tag{2}$$

It is noted here that $\hat{a}_1$ and $\hat{a}_2$ are not orthogonal to each other their inner products yield:

$$\hat{a}_1.\hat{a}_1 = \hat{a}_2.\hat{a}_2 = a^2; \qquad \hat{a}_1.\hat{a}_2 = \frac{a^2}{2} \tag{3}$$

where "a" is a lattice constant of honeycomb lattice and given by

$$a = a_{c\text{-}c}\sqrt{3} \tag{4}$$

where $a_{c\text{-}c}$ is the nearest neighbor distance between two carbon atoms in the lattice and numerically equal to 1.44 A°, so

$$a = 1.44A^\circ \times \sqrt{3} = 2.49A^\circ \tag{5}$$

If L be the circumferential length of the tube, tube diameter d_t is given by

$$d_t = \frac{L}{\pi} \tag{6}$$

where L can be obtained by using equations (1) and (3) as:

$$L = \left|\vec{C}_h\right| = \sqrt{\vec{C}_h.\vec{C}_h} = a\sqrt{n^2 + m^2 + nm} \tag{7}$$

hence, using (4), (6) and (7), the tube diameter is given by

$$d_t = \sqrt{3}a_{c-c}(n^2 + m^2 + nm)^{\frac{1}{2}} / \pi \tag{8}$$

For example, the diameter of armchair (5,5) is $d_t = 6.88\ A^{\circ}$.

(ii) The Chiral angle (θ)

The Chiral angle θ is defined as the angle between the vectors $\vec{C}_h$ and $\hat{a}_1$ with values of θ in the range $0^0 \le |\theta| \le 30^0$, because of the hexagonal symmetry of the honeycomb lattice. The Chiral angle θ denotes the tilt angle of the hexagons with respect to the direction of the nanotube axis, and the angle θ specifies the spiral symmetry. The Chiral angle θ is defined by taking the inner product of $\vec{C}_h$ and $\hat{a}_1$, to yield an expression for $(cos\ \theta)$ as:

$$\cos\theta = \frac{\vec{C}_h \cdot \hat{a}_1}{\left|\vec{C}_h\right|\left|\hat{a}_1\right|} = \frac{2n + m}{2\sqrt{n^2 + m^2 + nm}} \tag{9}$$

$$\sin\theta = \frac{\sqrt{3}m}{2\sqrt{n^2 + m^2 + nm}} \tag{10}$$

$$\tan\theta = \frac{\sqrt{3}m}{2n+m} \tag{11}$$

$$\theta = \tan^{-1}\left(\frac{\sqrt{3}m}{2n+m}\right) \tag{12}$$

(iii) The Number of hexagons "N", per unit cell of a chiral tube specified by integer (n, m) is given by

$$N = \frac{2(m^2 + n^2 + nm)}{d_R} \tag{13}$$

where d_R is given by

$$d_R = \begin{cases} d & \text{if n-m is not a multiple of 3d} \\ 3d & \text{if n-m is a multiple of 3d} \end{cases} \tag{14}$$

introducing "d" as the greatest common divisor (gcd) of n and m, and we note that each hexagon contains two carbon atoms. As an example, application of equation (13) to the (5,5) and (9,0) tubes yields values of 10 and 18 respectively, for N. These unit cells of the 1D tube contain, respectively, 5 and 9 unit cells of the 2D graphene lattice, each 2D unit cell containing two hexagons of the honeycomb lattice.

3.12 Synthesis Of Carbon Nanotubes

Carbon nanotubes can be made by laser vaporization synthesis method, carbon arc method, and chemical vapor deposition method. These methods are explained as follows.

(i) Laser Vaporization Synthesis Method

An efficient way for the synthesis of bundles of single-wall carbon nanotubes with a narrow diameter distribution employs the laser vaporization of graphite target. Figure 12 illustrates the apparatus for making carbon nanotubes by laser evaporation.

A quartz tube containing argon gas and a graphite target is heated to 1200°C. Contained in the tube, but somewhat outside the furnace, there is a water-cooled copper collector. The graphite target contains small amount of cobalt and nickel that act as catalytic nucleation sites for the formation of the tubes. An intense pulsed laser beam is incident on the target, evaporating carbon from the graphite. Flowing argon gas then sweeps the carbon atoms from the high temperature zone to the copper collector on which they condense into nanotubes. Tubes 10-20 nm in diameter and 100 μm long can be made by this method.

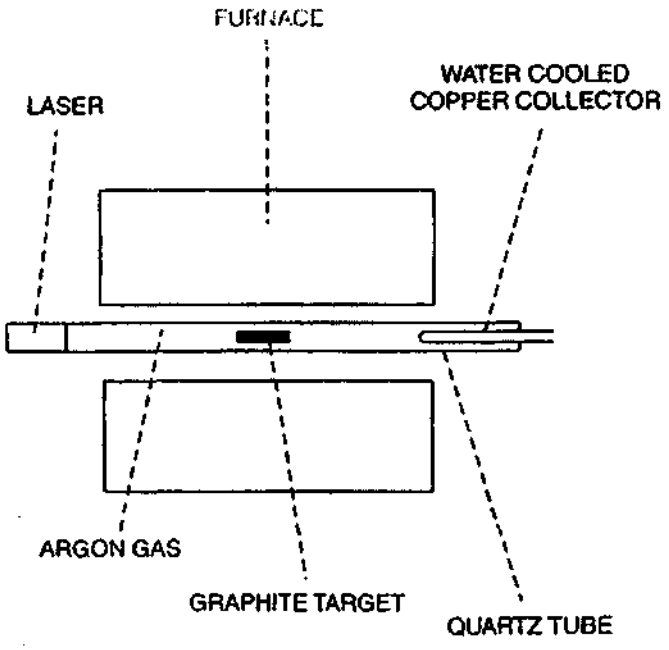

Figure 12. Experimental arrangement for synthesizing carbon nanotubes by laser evaporation.

(ii) Carbon Arc Method

The carbon arc provides a simple and traditional tool for generating the high temperature needed for the vaporization of carbon atoms into plasma (>3000°C)[23-24]. This technique has been used for the synthesis of single-wall and multi-wall carbon nanotubes [28]. The cross-sectional view of carbon arc generator to synthesize carbon nanotube is shown in Figure13.

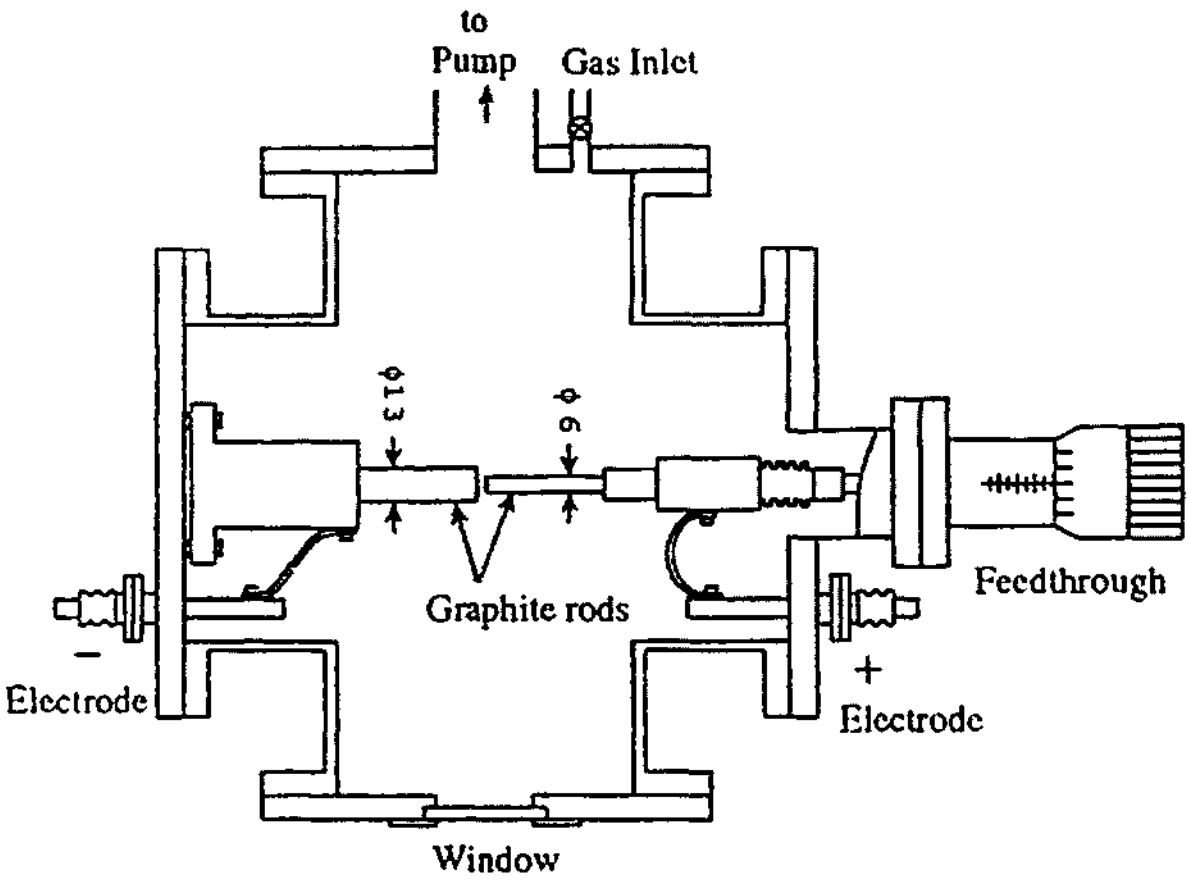

Figure 13. Cross-sectional view of a carbon arc generator that can be used to synthesize carbon nanotubes.

Typical conditions for operating a carbon arc for the synthesis of carbon nanotubes include the use of carbon rod electrodes of 5-20 mm diameter separated by ~1 mm with a voltage of 20-25 across the electrodes and a dc electric current of 50-120 A flowing between the electrodes. The arc is typically operated at 500- ~ torr pressure of flowing helium with a flow rate of 5-15 ml/s for cooling purpose. Carbon atoms are ejected from the positive electrode and form nanotubes on the negative electrode. As the tube forms, the length of the positive electrode decreases, and a carbon deposit forms on the negative electrode. For the multi-wall carbon nanotube synthesis, no catalyst need be used, but to produce single-wall carbon nanotubes, a small amount of cobalt, nickel or iron is incorporated as a catalyst in the central region of the positive electrode. This method can produce single-wall nanotube of diameters 1-5 nm with a length of 1 μm.

(iii) Chemical Vapor Deposition Method

The chemical vapor deposition method involves decomposing a hydrocarbon gas such as methane (CH_4) at 1100°C. As the gas decomposes, carbon atoms are produced that then condense on a cooler substrate that may contain various catalysts such as iron, cobalt and nickel. This method produced tubes with open ends, which does not occur when other methods are used. This procedure allows continuous fabrication, and may be the most favorable method for scale up and production.

(iv) Other Synthesis Method (Ion Bombardment Technique)

Another method of nanotube synthesis relates to the use of carbon ion bombardment to make carbon whiskers [29]. Carbon whiskers are known as a graphite material with crystallinity whose diameter is ~ 0.1-1 μm and several mm in length. In the ion bombardment technique, carbon is vaporized in vacuum through ion or electron irradiation, and the resulting deposit containing carbon nanotubes, along with other structures is collected on a cold surface. Little is known about the optimization of the ion bombardment technique in relation to the preparation of nanotubes.

3.13 Electrical Properties

Carbon nanotubes have the most interesting properties that they are metallic or semiconducting, depending on the diameter and chirality of the tube. Synthesis generally results in a mixture of the tubes two third of which are semiconducting and one third metallic. The metallic tubes have the armchair structure shown in Figure 11(a). In the metallic state the conductivity of the nanotubes is very high. It is estimated that they can carry billion amperes per square centimeter. Copper wire fails at one million amperes per square centimeter because resistive heating melts wire. One reason for the high conductivity of the carbon nanotube is that they have very few defects to scatter electrons, and thus a very low resistance. High currents do not heat the tubes in the same way that they heat copper wires. An important result pertaining to semiconductor nanotubes, shows that their energy gap depends upon the reciprocal nanotube diameter d_t:

$$E_g = \frac{|t| a_{c-c}}{d_t} \tag{15}$$

independent of the chiral angle of the semiconducting nanotube, where $a_{c-c} = a/\sqrt{3}$ is the nearest neighbor C-C distance on a graphene sheet, and $|t|$ is the nearest neighbor C-C tight binding overlap energy. Equation (15) indicates that as the diameter of the tube increases, the band gap decreases.

3.14 Mechanical Properties

Carbon nanotubes are very strong. They have Young's moduli ranging from 1.28 to 1.8 TPa [2]. One terapascal (TPa) is a pressure very close to 10^7 times atmospheric pressure. Young's modulus of steel is 0.21TPa, which means that Young's modulus of carbon nanotube is almost 10 times that of steel. This would imply that carbon nanotubes are very stiff and hard to bend. However, this is not quite true because they are so thin.

When carbon nanotubes are bent, they are very resilient. They can be straightened back without any damage, because they have so few defects in the structure of their walls. Another reason why they do not fracture is that as they are bent severely, the almost hexagonal carbon rings in the walls change in structure but do not break. This is a unique result of the fact that the C-C bonds are sp^2 hybrids, and these sp^2 bonds can rehybridize as they are bent.

Strength is not the same as stiffness. Young's modulus is measure of how stiff a material is. Tensile strength is a measure of the amount stress needed to pull a material apart. The tensile strength of carbon nanotubes is about 45 billions pascals. High strength steel alloys break at about 2 billion pascals. Thus carbon nanotubes are about 20 times stronger than steel.

3.15 Applications Of Carbon Nanotubes

(i) MOSFETs (CNTFETs)

A CNTFET is the analogue of silicon MOSFET in which SWCNTs replace the silicon channel. The feasibility of designing field-effect transistor (FETs), the switching components of computers, based on semiconducting carbon nanotubes connecting two gold electrodes, has been demonstrated. An illustration of the device is shown in Figure 14. When a small voltage is applied to the gate, current flows through the nanotube between the source and drain. It has been found that a small voltage applied to the gate can change the conductivity of the nanotube by a factor of $> 1x10^6$, which is comparable to Si-Field Effect Transistor. It has been estimated that the switching time of these devices will be very fast, allowing clock speed of a terahertz, which is 10^4 times faster than present processors.

With respect to FETs, nanotubes do not have surface dangling bonds, as silicon does, and so there is no need to mainly use silicon dioxide (SiO_2) as the gate insulator.

Other crystalline or amorphous insulators with higher dielectric constants can be used instead. This implies that one can get higher performance in CNTFETs without having to use ultra thin SiO_2 gate insulating films. In addition, CNTFETs may make new applications possible. For example, semiconducting SWCNTs, unlike silicon, are direct-gap materials and, as such, they directly absorb and emit light, thus possibly enabling a future optoelectronics technology based on SWCNTs.

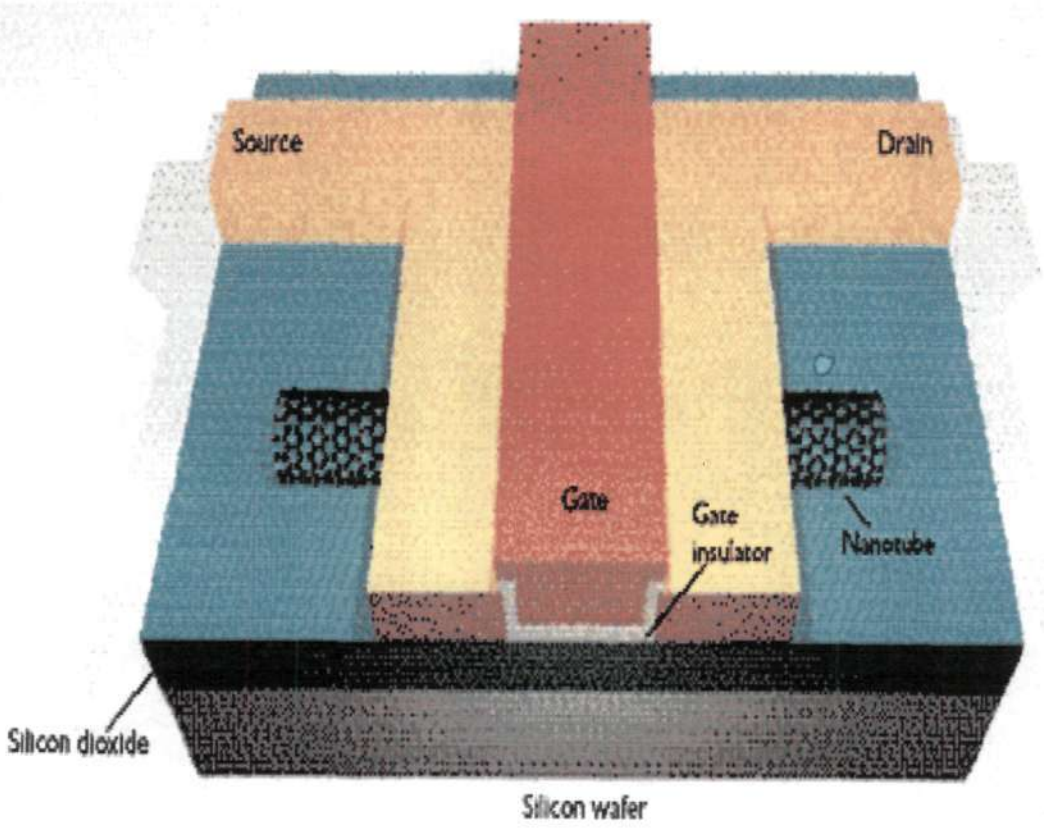

Figure 14. Illustration of CNTFET

(ii) Battery Technology

Carbon nanotube have applications in latest battery technology. Lithium, which is a charge carrier in some batteries, can be stored inside nanotubes. It is estimated that one lithium atom can be stored for every six carbons of the tube. Storing hydrogen in nanotubes is another possible application.

(iii) Field Emission

Carbon nanotubes have field emission effect. One application of this effect is the development of flat panel display. Samsung company in Korea is developing a flat panel display using the electron emission of carbon nanotube. A Japanese company is using this electron emission effect to make vacuum tube lamps that are as bright as conventional light bulbs, and longer-lived and more efficient.

(iv) Catalysis

Nanotube serve as catalysts for some chemical reactions, chemical reactions have also been carried out inside nanotubes. For example, Cadmium Sulfide (CdS) crystal has been formed in side nanotubes by reacting Cadmium Oxide (CdO) crystal with hydrogen sulfide gas (H_2S) at 400°C.

Final Remark

Keeping in views the unique electrical and mechanical properties, it can be concluded that carbon nanotubes are very attractive to both fundamental science and technology. The applications discussed earlier, will, of course, require inexpensive bulk fabrication of nanotubes.

References

1. Dresselhaus, M. S., Dresselhaus, G. and Saito, R., "Nanotechnology in carbon materials" in Nanotechnology, G.Timp, ed., Springer-verlag, 1998, chapter 7, p.285.
2. Charles P. Poole, Jr. Frank J. Owens, Carbon Nanostructure, in "Introduction to Nanotechnology" 2003, chapter 5, p.103.
3. Dresselhaus, M. S., Dresselhaus, G. and Eklund, P. C., J. Mater. Res. 8, 2054 (1993).
4. Kroto, H.W., et al. Nature (London) 318, 162-163 (1985).
5. Stephens , P. W. , et al. Nature (London) 351, 632 (1985).
6. Jonshon, R.D., Bethune, D.S., and Yannoni, C. S., Accounts chem., Res. 25, 169 (1992).
7. Dresselhaus, M. S., Dresselhaus, G. and Eklund, P. C., Science of Fullerenes and carbon Nanotubes, NewYork: Academic Press, 1995.
8. Rohlfing, E.A., Cox, D. M. and Kaldor, A., J. Chem. Phys. 81, 3322 (1984).
9. Haddon, R. C., et al., Nature (London) 350, 320 (1991).
10. Hebard, A.F., Physics Today 45, 26 (1992).
11. Dresselhaus, M. S., Dresselhaus, G., Advances in Physics. 30, 139-326 (1981).
12. Rosseinsky, M. J., et. al., Nature (London) 352, 416 (1992).
13. Tanigaki, K., et al., Nature (London) 352, 222 (1991).
14. Herold, A., in physics and chemistry of materials with Layered structures, Levy, F., ed., New York: Dordrecht Reidel, 1979, p. 323.
15. Datars, W.R. et al., Solid State Commun. 86, 579-582 (1993).
16. Datars, W.R. et al., Phys. Rev. B 50, 4937 (1994).
17. Smalley, R.E. Mater. Sci. Eng. 319, 1-7 (1993).
18. Palstra, T.T.M., et al., Solid State Commun. 93, 327 (1995).
19. Hebard, A. F., Physics Today 29 (Nov. 1992).

20. Bethure, D. S., et al., Nature (London) 366, 123 (1993).
21. Stephens, P. W., et al., Nature (London) 351, 632 (1991).
22. Iijima, S., Nature (London) 354, 56 (1991).
23. Ebbesen, T. W. and Ajayan , P.M. Nature (London) 358, 220 (1992).
24. Ebbesen, T.W., et al., Chem. Phys. Lett. 209, 83 –90 (1993).
25. Dresselhaus, M.S., Dresselhaus, G., and Saito, R., Phys. Rev. B45, 6234 (1982).
26. Saito, R., et al., Appl. Phys. Lett. 60, 2204 (1992)
27. Saito, R., Dresselhaus, G. and Dresselhaus, M.S., "Physical Properties of carbon Nanotubes", Imperical college Press. 2003, Chapter 3, p35.
28. Journet, C., Maser, W.K., Bernier, P., Loiseau, A., Lamy, M., de la Chappele, Lefront, S., Deniard, P., Lee, R., and Fisher, J.E. Nature (London) 388, 756 (1997).
29. Cuomo, J.J., and J.M., Harper, E. IBM Tech. Disclosure Bulletin 20, 775 (1977).

Chapter 4

Analysis of Carbon Nanotube Based Nanodevices

Chapter 4

Analysis Of Carbon Nanotube Based Nanodevices

Carbon nanotube [1] constitute a fascinating new class of materials with a broad range of potential applications. Recently the research of carbon nanotubes (CNTs), narrow seamless graphene cylinders with nanometer-size diameter and millimeter-size length as constituents of nanoscale materials and structure, has attracted much attention. They are predicted to have unprecedented potential practical applications in nano-electronics for developing nano-electronic devices.

A scanning tunneling microscope (STM) is used to explore the local electrical characteristics of single-wall carbon nanotubes (SWCNTs). By moving the STM tip along the length of the nanotubes well defined positions can be found where the transport current changes abruptly from a graphite-like response to one that is highly nonlinear and asymmetrical, including near perfect rectification.

Electronically, nanotubes are expected to behave as ideal one-dimensional (1D) "quantum wires" with either semiconducting or metallic behaviors, depending on geometrical tube parameters [2-4]. The joining of dissimilar tubes could result in non-linear junction devices formed from only a handful of carbon nanotubes (see Figure 1).

It has been suggested that localized defects, such as pentagon-heptagon pairs, can be the basis of nanoscale nanotube devices [5-8]. Individual single-wall carbon nanotubes (SWCNTs) can act as conducting quantum wires, single-electron tunneling transistors (SETs), and spin electronic devices [9-12]. It can also be used as a conducting channel connecting the drain and source electrode in a MOSFET (CNTFET). A combination of nanotubes can act as rectifiers [13] or more complex multi-terminal devices [14].

However, for rational design of these devices, it requires a fundamental understanding of the electrical and magnetic properties of CNTs and how they depend on their structural parameters such as the diameter, number of concentric shells, chirality of tubes etc. Some carbon nanotube based nanodevices are:

A. Nanotube Junction

4.1 Net Diagram Of A Nanotube Junction

Connecting two single-wall carbon nanotubes is an interesting problem, since a semiconductor-metal junction is realized by connecting a semiconductor and a metal carbon nanotube. In Figure 1, the junction between two carbon nanotubes with different diameters is shown. In this Figure the larger diameter carbon nanotube AB is joined to a smaller diameter nanotube CD through a junction section BC containing a single size pentagon B and a single heptagon C.

In Figure 1, we show examples of (a) (12,0)-(9,0) and (b) (12,0)-(8,0) zigzag nanotube junctions, in which the carbon atoms of the pentagon and the heptagon rings are indicated by filled circles. All the other polygons in the nanotube junction are hexagons. All carbon atoms in the junction have three σ sp^2 covalent bonds, and there are no sp^3 covalent bonds in the junction. Thus we can say that the pentagon and heptagon defects are topological point defects, associated with the joining of the two nanotubes. The positive curvature of the pentagonal ring, as is generally seen in fullerenes, makes the diameter of carbon nanotube decrease in going from left to right and the negative curvature of the heptagonal ring prevents further decrease in the nanotube diameter. Thus, when the difference between the diameters of the two carbon nanotubes becomes large, the distance between the pentagon and heptagon also becomes large.

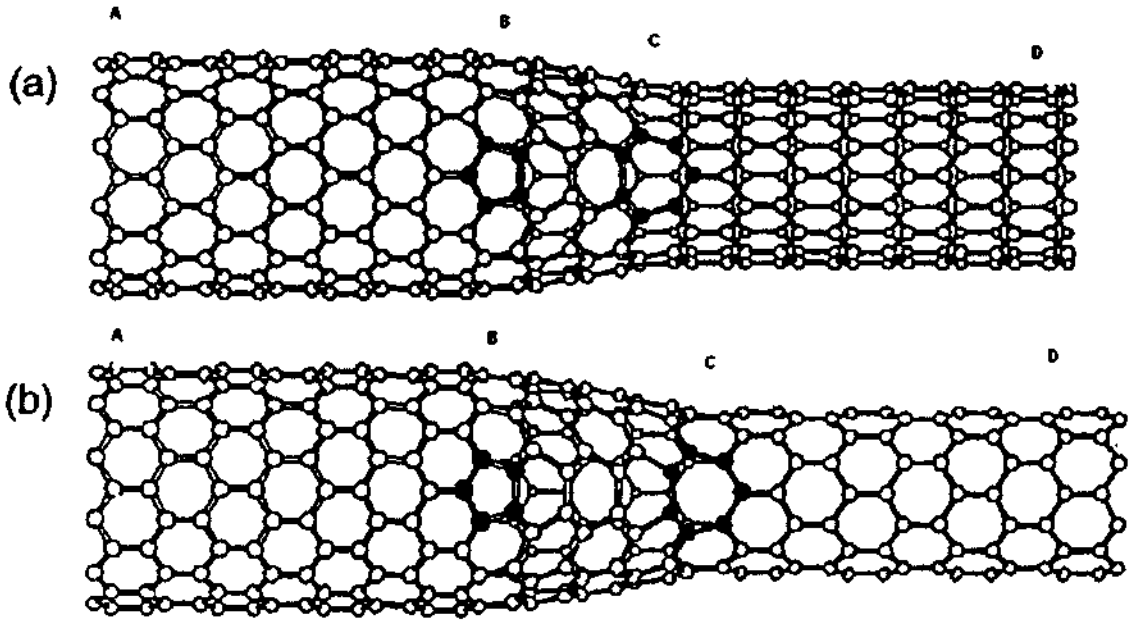

Figure 1. Junctions of (a) (12,0) - (9,0) and (b) (12,0) – (8,0) zigzag nanotubes are shown in which the carbon atoms of the pentagon and the heptagon are indicated by filled circles.

To describe a junction formed by connecting two carbon nanotubes of different geometries [i.e. described by different chiral vectors (n, m)], a net diagram is used. In Figure 2, a net diagram of a nanotube junction is shown, in which two carbon nanotubes are given by the rectangles TABU and RCDS. The smaller tube TABU and the larger tube RCDS, are uniquely determined by the chiral vectors, $\vec{AB}$ and $\vec{CD}$, respectively. Here a pentagon exists at the site C (or D) and a heptagon exists at A (or B). Since the solid angles of a pentagon and a heptagon in the fullerene are $\left(2\pi'-\frac{\pi}{3}\right)$ and $\left(2\pi+\frac{\pi}{3}\right)$, respectively, the sum of the angle on the net diagram around the pentagon and the heptagon, indicated by shaded hexagons, should correspond to these angles. This fact gives the angle relation:

$$\left.\begin{aligned} \angle ACR + \angle BDS &= 2\pi - \frac{\pi}{3} = \frac{5\pi}{3}, \\ \text{and} \qquad \angle CAT + \angle DBU &= 2\pi + \frac{\pi}{3} = \frac{7\pi}{3} \end{aligned}\right\} \qquad (1)$$

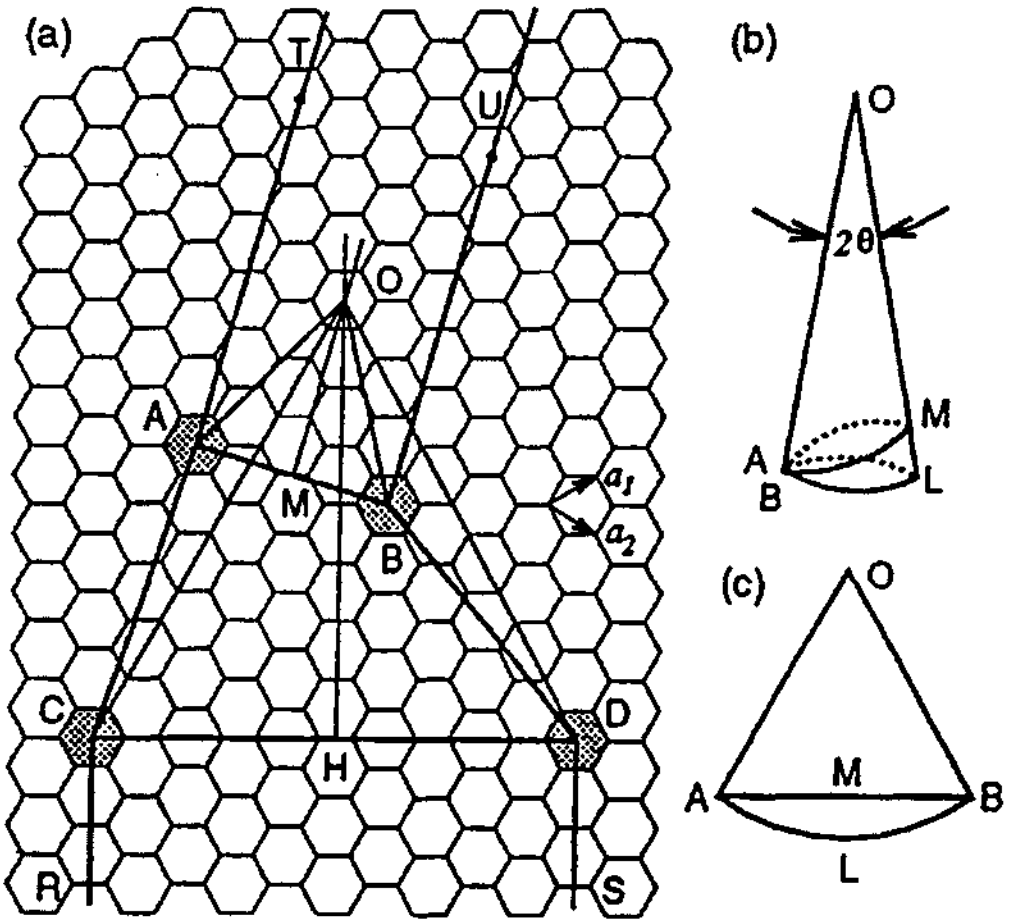

Figure 2. (a) Net diagram for the joint between two nanotubes. The chiral vectors for the two nanotubes are shown by $\vec{AB}$ and $\vec{CD}$. (b) The cone of OALB and (c) its projection is shown for understanding that the line AMB is a line of minimum length for going around the surface of the cone.

The three dimensional (3D) structure is obtained by connecting AT to BU, AC to BD, and CR to DS through cylindrical surfaces. When we roll up the net diagram to make a tube, the chiral vectors $\overline{A}\vec{B}$ and $\overline{C}\vec{D}$ correspond to the circumferential directions of the tubes while the translation vectors $\overline{A}\vec{T}$ and $\overline{C}\vec{R}$ which are perpendicular to $\overline{A}\vec{B}$ and $\overline{C}\vec{D}$, respectively, corresponding to the directions of the nanotube axes in three dimensions.

4.2 Geometrical Analysis

When side AC is connected to BD in Figure 2, using equation (1), we get:

$$\left.\begin{aligned} &\angle ACD + \angle BDC = \frac{2\pi}{3} \\ \text{and,} \quad &\text{AC} = \text{BD} \end{aligned}\right\} \qquad (2)$$

then $\overline{B}\vec{D}$ is given by first rotating $\overline{A}\vec{C}$ around C by $\pi/3$ and then translating by $\overline{C}\vec{D}$. Thus, we can connect two carbon nanotubes to form nanotube junction satisfying equation 2.

The polygon, ACDB, in the net diagram [Figure 2 (a)] denotes the joint , which connects the two nanotubes. The shape of the joint provides the shape and axes of the cone as shown in Figure 2(b) and (c). For the cone, OALB, the line AMB is a line of minimum length for going around the surface of cone, in which OM perpendicular to AMB satisfies both Figures 2(b) and (c). We assume here that the line AMB and CHD in Figure 2 (a) correspond to the minimum lines of the cone surface. This assumption is also satisfied for the two tubes, TABU and RCDS, when the lines AMB and CHD are minimum in length for going around the nanotube surface. ACDB is a part of cone whose vertex is denoted by O in Figure 2(a). The vertex of the cone, O, is defined as the

crossing of the two lines OM and OH such that OM and OH are perpendicular bisectors of AB and CD, respectively. In three dimensions, the angle of the vertex of the cone is defined as 2θ, as shown in Figure 2(b), where θ is given by

$$\theta = Sin^{-1}\left(\frac{1}{6}\right) \approx 9.594^{\circ} \qquad (3)$$

the angle θ is the angle between the axes of the tube and the axes of the cone in three dimensions. If points O, B, and D [in Figure 2(a)] lie on a line, the angle between the two axes of the tubes becomes zero, but when the pentagon and heptagon are on the opposite sides of the cone surface, then the angle between the two axes of the tube becomes $2\theta = 2\times 9.594 = 19.19^{\circ}$ [15].

Here we mention that the path AMB is an ellipse on the cone surface in three dimension [Figure 2(b)], while the path AMB is a circle on the nanotube surface. Thus we can always expect some distortion arising from the elliptical shape of the cone section relative to the circle shape of the nanotube surface.

If we denote the major and minor axes of the ellipses as "a" and "b", the ratio of "b" to "a" is given as a function of θ. After some calculation, b/a is given by:

$$\frac{b}{a} = \left(1 + \frac{4}{3}Sin^2\theta - \frac{2\sqrt{3}}{3}\tan\theta\right)^{1/2} \qquad (4)$$

using the value of θ from equation (3), we get:

$$\frac{b}{a} \sim 0.918$$

thus the cross section of the circle at the end of the nanotube is distorted by (1-0.918) = 0.82 = 8.2% distortion at the junction. But this distortion will not affect the angle on the tube or cone surface, because the distortion is perpendicular to the surface.

4.3 Tunneling Conductance Of Nanotube Junction

Figure 3 shows the conductance I/V for the carbon nanotube junctions of Figure 1(a) (12,0) – (9,0) and (b) (12,0) – (8,0) zigzag nanotubes. The plots for conductance in Figure 3 are made as a function of applied voltage V/t (-0.5 < V/t < 0.5), for two different Gaussian broadening values, $\Delta E / t = 0.33$ (solid lines) and $\Delta E / t = 0.50$ (dotted lines).

For metallic – metallic nanotube junction [Figure 3(a)], the conductance increases with increasing applied voltage. The oscillations in the conductance show resonances in the tunneling probability between the two nanotubes. The increase of the conductance with increasing V comes from the fact that the resonance tunneling probability is proportional to V, if the density of states is constant near the fermi energy. Again we mention that there is no contribution to the conductance from the edge states, which can be automatically excluded because their wave functions have no amplitude in the junction region. Here we assume that it is only in the junction region that we expect a voltage drop. Since this nanotube junction system is so small, we consider the carbon network to be in the mesoscopic regime, in which electrons are scattered only in the junction region. Tunneling current appears when the energy of the wave function to the left of the junction coincides with the energy plus eV of that to the right.

For a metal – semiconductor nanotube junction [Figure 3(b)], there is no conductance in the energy gap region for the semiconducting (8,0) nanotube. Since in the case of the metal – semiconductor (12,0) – (8,0) zigzag nanotubes, the density of states near the fermi energy is smaller than that of the (12,0) – (9,0) system because of the absence of a finite density of states for the (8,0) carbon nanotube near the fermi energy.

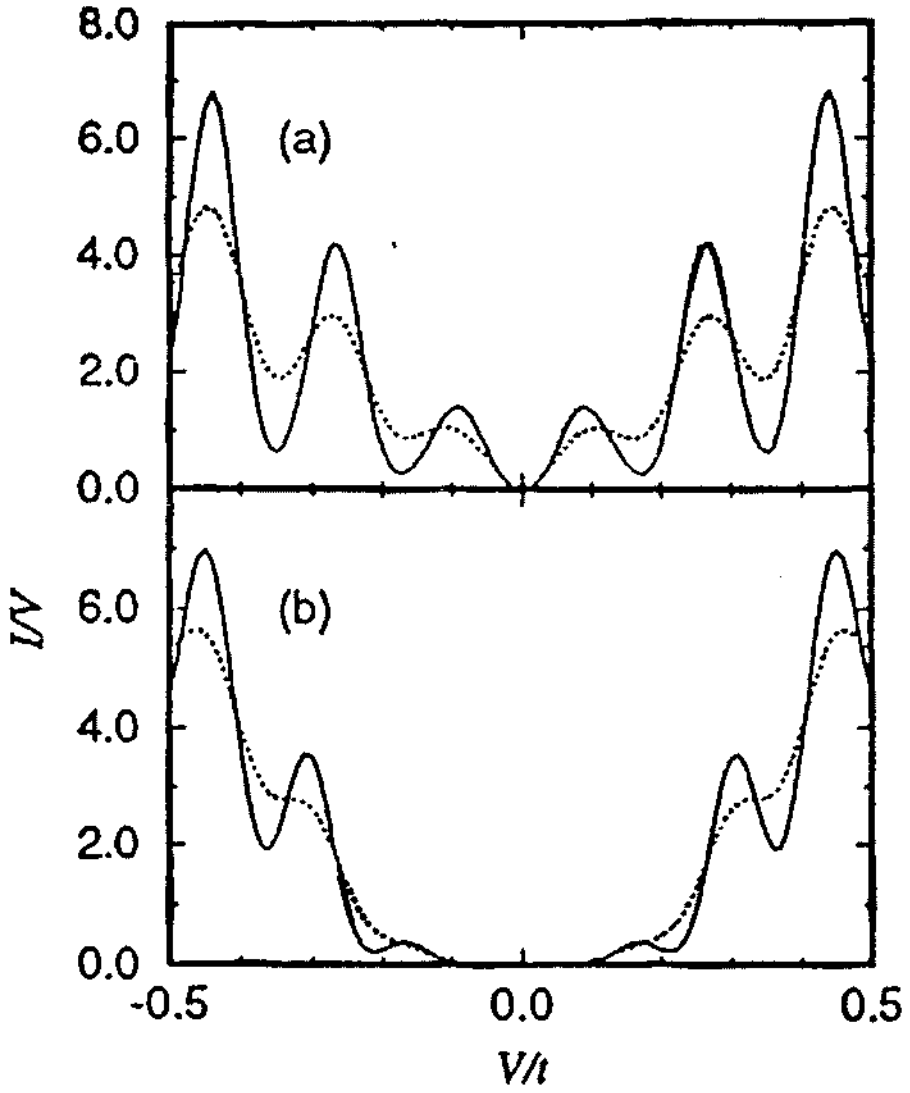

Figure 3. Calculated conductance I/V for (a) (a) (12,0) - (9,0) and (b) (12,0) – (8,0) zigzag nanotubes junction as a function of voltage V in units of $|t|$, using two different gaussian broadening values.

The results clearly show that delocalized wave function is present near the fermi level only in the metallic nanotube region. Thus it is concluded that a metal – semiconductor nanotube junction is well established even in a nanoscale, mesoscopic structure.

B. Schottky Diode

(STM metal tip – carbon nanotube system)

Under this heading, we analyze a model for observed current voltage (I-V) characteristics in an experiment with a scanning tunneling microscope (STM) tip and a carbon nanotube [13], which was carried out at room temperature by "Toshishige Yamada" in NASA Ames research center, California.

4.4 Experimental Procedure

To observe current – voltage (I-V) characteristic, the STM tip was driven forward into a film of many entangled nanotubes on a substrate, and then was retracted well beyond the normal tunneling range, as shown in Figure 4(A) and (B).

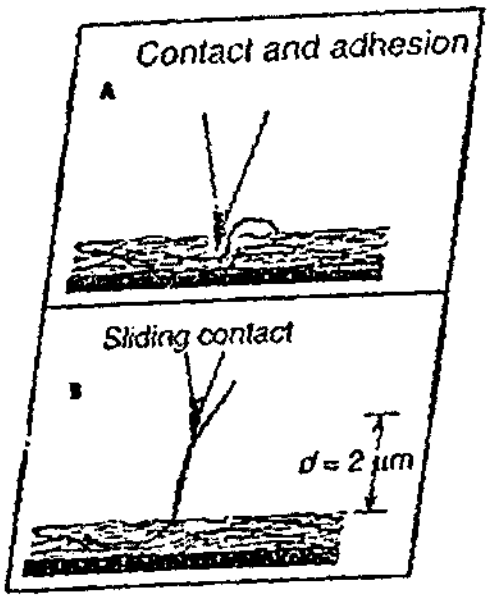

Figure 4. Schematic of the procedure for measuring nanotube characteristic with a single STM tip.

At a distance of ~0.1μm above the surface, there was usually electronic conduction between the tip and the film since nanotubes bridged the two regions. At ~ 2 μm, only one nanotube remained occasionally [as shown in Figure 4(B)], and the electronic conduction was still maintained. One end of the nanotube continued sticking to the tip during retraction, while the other consistently stayed in the film. I-V characteristics for this tip – nanotube system showed rectification, i.e., $I \neq 0$ only with $V < 0$, if the tip was grounded, as shown in Figure 5, 6,7, and 8.

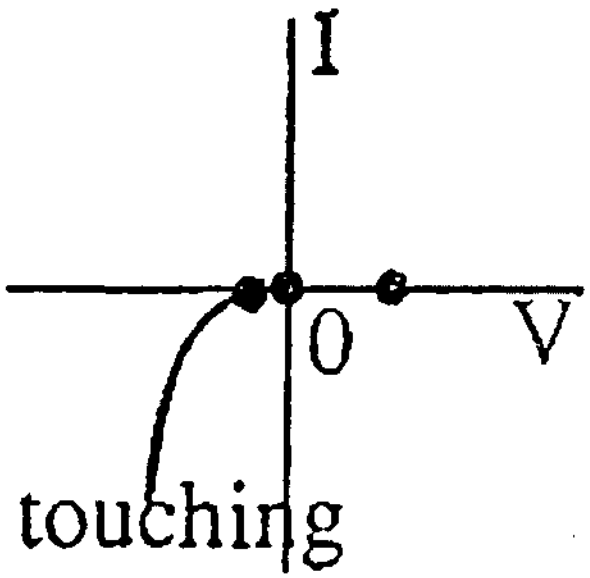

Figure 5. I-V characteristic for STM tip- CNT system experimentally.

We consider that the observed characteristics strongly the nature of the tip (metal) – nanotube (semiconductor) contact. The other end of the nanotube was entangled well

into the film, and simply provided good ohmic contact. Experimentally, the tip was not placed at the end of the nanotube, but contacted the side of the nanotube so that the tip and nanotube surfaces faced each other. Therefore, the tip – nanotube junction s approximated well by the traditional planer junction model [16].

4.5 Band Diagrams For STM tip – Nanotube System

The band diagrams for tip – nanotube system are shown in following figures.

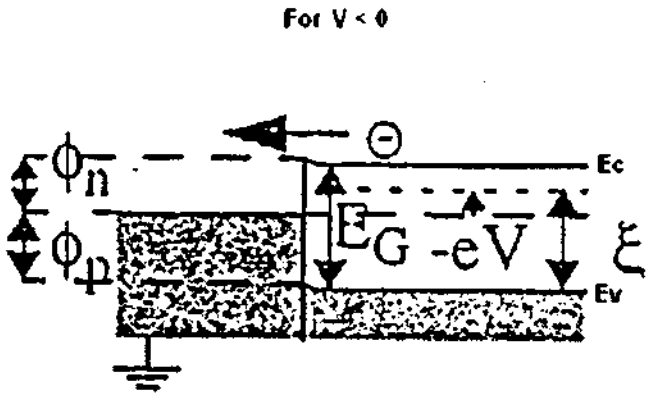

Figure 6. Schottky forward with V < 0.

Where Φ_n and Φ_p are schottky barriers, E_G is the energy band gap and $\xi = E_{FS} - E_v$, E_{FS} is the fermi energy, and E_c and E_v are conduction and valance band edges, respectively, and depend on the applied voltage V after the tip is grounded. From Figure 5 and 6, it follows that $I \neq 0$ only with V < 0, and the nanotube has be n type semiconducting in nature.

For V = 0

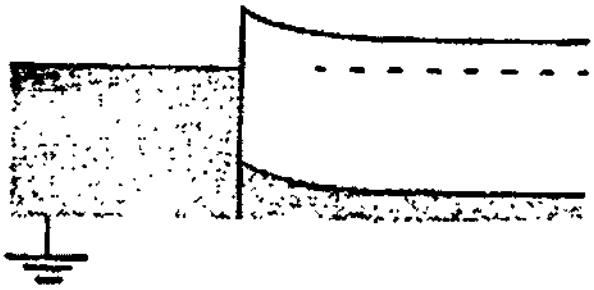

Figure 7. Equilibrium condition with V =0.

For V > 0

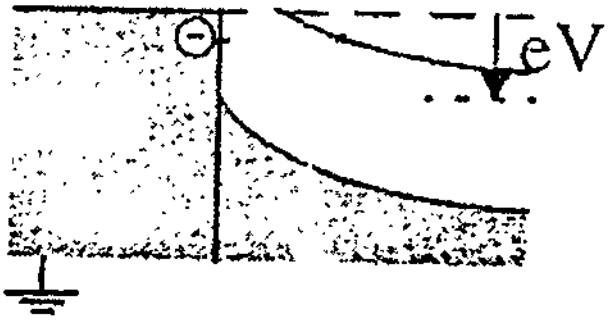

Figure 8. Schottky reverse with V > 0.

Figure 8 shows a reverse condition with V > 0 with negligible current. We note that for p type semiconducting nanotubes, the entire I- V pattern simply shifts to the positive V direction.

Explanation

(1) Under no biasing (V=0), no current is observed (equilibrium condition, Figure 7).

(2) When we apply a positive voltage (V > 0) to the semiconductor with respect to metal barrier height increases, while schottky barrier remains constant in this idealized case. This bias condition is reverse bias, as shown in Figure 8.

(3) The current mechanism here, however, is due to the flow of majority carrier electrons. In forward bias (V < 0), the barrier seen by electrons in the semiconductor is reduced, so majority carriers flow more easily from semiconductor to metal, as shown in Figure 6. The forward bias current is in the direction from metal to semiconductor. It is an exponential function of the forward bias voltage.

4.6 Theoretical Analysis

The nanotube used in the experiment was of the diameter 1.36 nm. Let us check the behavior of the tube used in the experiment as follows:

We consider a nanotube having chirality (17,0), so obviously

$$n = 17$$
$$m = 0$$

The diameter of nanotube is calculated as:

$$d_t = \frac{L}{\pi},$$

here L is circumferential length and is given by:

$$L = \left|\vec{C}_h\right| = \sqrt{\vec{C}_h.\vec{C}_h} = a\sqrt{n^2 + m^2 + nm}$$

where "a" is a lattice constant of honeycomb lattice and numerically equal to 2.49 A°.

Hence, for a nanotube used in the experiment, the circumferential length is 4.233 nm, and the diameter is 1.34 nm, the closest value to the experimental value (i.e. 1.36 nm). The chirality $(n,0) \equiv (17,0)$ implies that the nanotube used in the experiment has trans type shape of its cross- section belonging to zigzag tube families and is semiconducting in nature [17,4].

The STM tip was of the tungsten having work function of 4.5 eV.

The diode current is given by:

$$I_D = -I_o[\exp(-\beta V_D) - 1]$$

Where V_D = diode voltage

β= inverse temperature (= 1/kT) ~38.61/eV

I_o = maximum current and is given by:

$$I_o = SA^*T^2 \exp(-\beta\phi_n)$$

where S = STM tip – nanotube overlap area ~0.1 nm^2

A^* = Richardson constant ~ 10 $A/cm^2/K^2$

T = Room temperature (~300 K)

Φ_n = Schottky barrier ~ 0.5 eV (< Eg ~ 0.54 eV)

Using the data mentioned above, we get:

$$I_o = 3.6 \times 10^{-18} A$$

Which agrees with the experimental value.

We calculate range of I_D for STM tip- CNT system using V_D ranging from –1V to +1V in steps 0.25, as:

V_D	I_D
-1	-21.096e-2
-0.75	-13.428e-6
-0.50	-8.604e-10
-0.25	-5.544e-14
0	0
0.25	3.564e-18
0.50	3.564e-18
0.75	3.564e-18
1	3.6e-18

The Current- Voltage (I-V) characteristic for STM tip – CNT system is shown below:

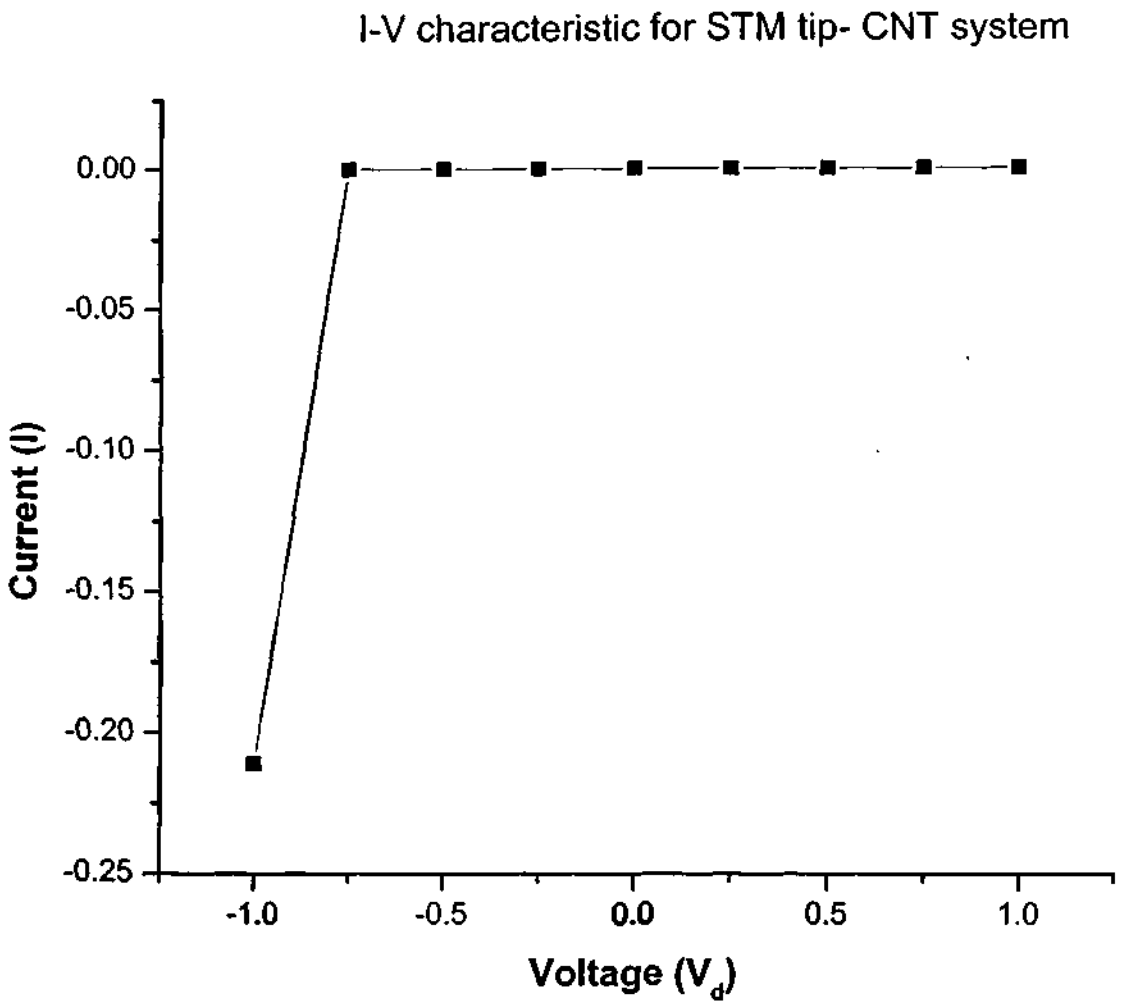

Figure 9. The I-V characteristic for STM tip – CNT, calculated with the Schottky formula.

For further investigation, S, Φ_n, and A^* need to be determined experimentally.

C. CNTFET (Carbon Nanotube Field Effect Transistor)

Over the past few years, critical dimensions of silicon MOS devices have decreased dramatically. Prototype transistors with gate length in 30- nm range have been successfully fabricated and were found to exhibit excellent electrical characteristics. While there is still some room for further improvements, the consensus is that alternative concepts will become necessary at some point in future. Among the materials investigated to date, carbon nanotubes field effect transistors (CNTFETs) are one of the most promising candidates for future nanoelectronics.

With the end of silicon transistors scaling, a great deal of research activity is currently focused on identifying alternatives which would enable continued improvements in the density and performance of electronics information systems. Other alternatives for more density and performance of electronics information systems are high-dielectric-constant (high-k) gate dielectric, metal gate electrode, double-gate FET, and strained-Si FET. High dielectric-constant materials are useful as gate insulators as they can provide efficient charge injection into transistor channels and reduce direct tunneling leakage currents. Of the various materials systems and structures being investigated carbon nanotubes have shown the promising characteristics. Carbon nanotubes are hollow seamless cylinders that can be envisioned as being formed by rolling up a finite sized piece of graphite sheet. Depending on how the roll-up of the graphite sheet occurs during the growth process, carbon nanotubes can exhibit semiconducting as well as metallic character. Moreover, the band gap of the semiconducting tubes scales inversely with the tube diameter. The growth process can be tuned such that fine control of the tube diameter is achieved thereby forming semiconducting tubes with very similar electrical properties. Growth conditions giving

the best yield produce carbon nanotubes with a diameter of around 1.4nm [18] resulting for semiconducting tubes in an energy gap of 0.6 eV.

With respect to electronics applications the small tube size implies that a high packing density of tubes in an array can be achieved in principle. On the other hand, the existence of metallic as well as semiconducting nanotubes points towards a fully carbon nanotubes-based electronics where metallic tubes act as interconnecting wires and semi conducting tubes work as active device elements. However, the most important aspect in view of the electrical properties of carbon nanotubes is their one-dimensional (1dim) character. Carbon nanotube field effect transistors (CNTFETs) are particularly attractive due to novel device physics.

4.7 Structure Of CNTFET

The Top-gated carbon nanotube field-effect transistors (CNTFETs) have the structure similar to that of conventional silicon metal- oxide semiconductor field- effect transistors (MOSFETs) with gate electrodes above the conduction channel separated from the channel by a thin (15-20 nm) SiO_2 dielectric, as shown schematically in Figure 14 in chapter 3. Top gate CNTFETs, which locate a gate electrode on top of a CNT, are advantageous because they can control the carrier density in a specific region. A CNTFET is the analogue of silicon MOSFET in which SWCNTs replace the silicon channel. A CNTFET consists of a SWCNT bridging two electrodes (source and drain). For imaging, an atomic force microscopy (AFM) is used in the non-contact mode.

Figure 10 shows the AFM image of CNTFET. A CNT is positioned on a silicon substrate covered by a SiO_2 film. The source, gate, and drain electrodes are sequentially located on CNT. Each of these electrodes keeps sufficient distance (~ 400 nm) from each other to minimize the influence of the gates on the Schottky barriers, which may exist at

the source and darin. The distance between the source and drain is 1μm. The gate length is 210 nm [19].

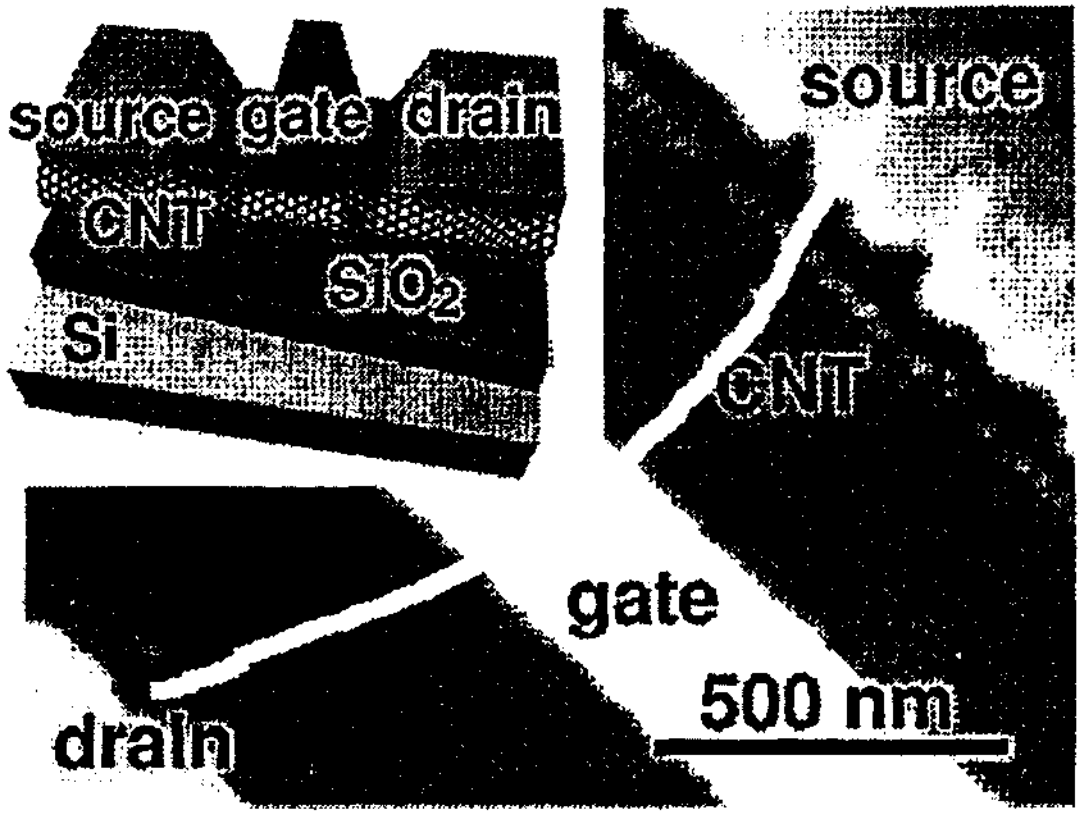

Figure 10. An AFM image of a CNTFET in which an individual CNT bridges the 1 μm gap between the source and darin electrodes.

4.8 I-V Characteristics Of CNTFET

Figure 11 shows drain current I_D as a function of drain voltage V_{DS} for a CNTFET with a CNT diameter of 1.5 nm. Gate voltage V_G applied on the top gate is swept from –0.6V to 0.6V in steps of 0.2V. Drain voltage V_{DS} is swept in the range $-1V < V_{DS} < 0V$. `Substrate voltage V_{SUB} is set to zero, $V_{SUB} = 0V$. Drain current I_D at $V_G = -1V$ depends on V_{DS} almost linearly and reaches as ~7.5 μA at $V_{DS} = -1V$. Drain current I_D decreases as V_G increases, similar to conventional p-type depletion-mode MOSFETs.

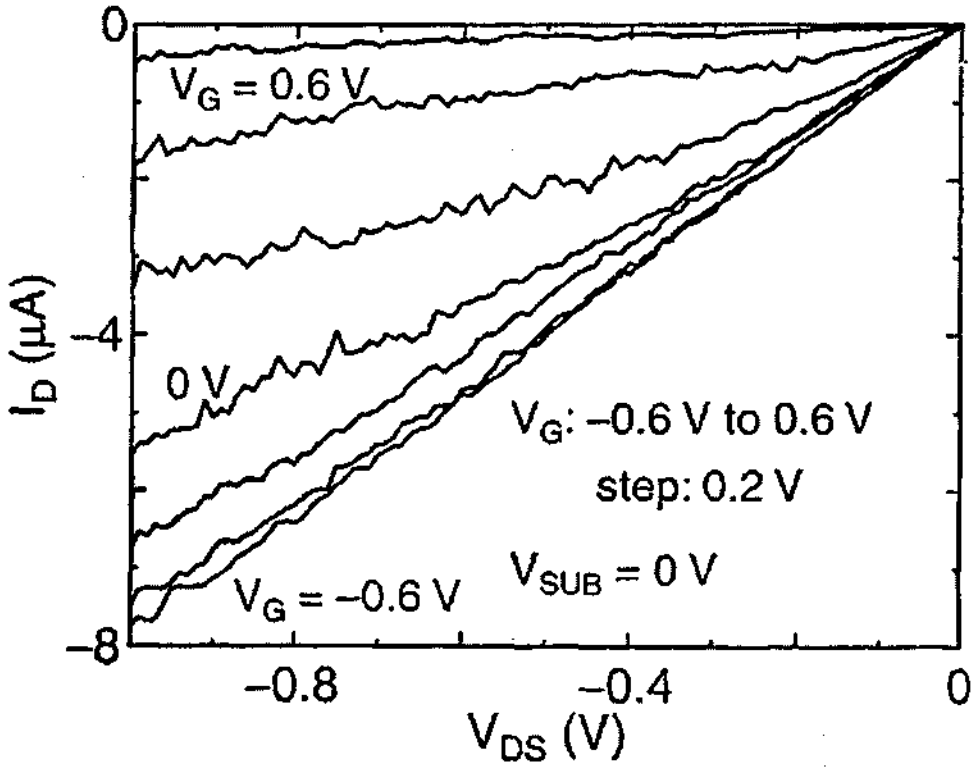

Figure 11. I_D as a function of V_{DS} for CNTFET with a CNT diameter of 1.5 nm.

Figure 12 shows a function of V_G at V_{DS} = -1V and V_{SUB} = 0V. Drain current I_D is suppressed ($I_D \approx 0$) for $V_G > 0.7V$. For $V_G < 0.5V$, I_D increases as V_G decreases. Especially, I_D depends linearly on V_G for $-0.2V < V_G < 0.5V$.

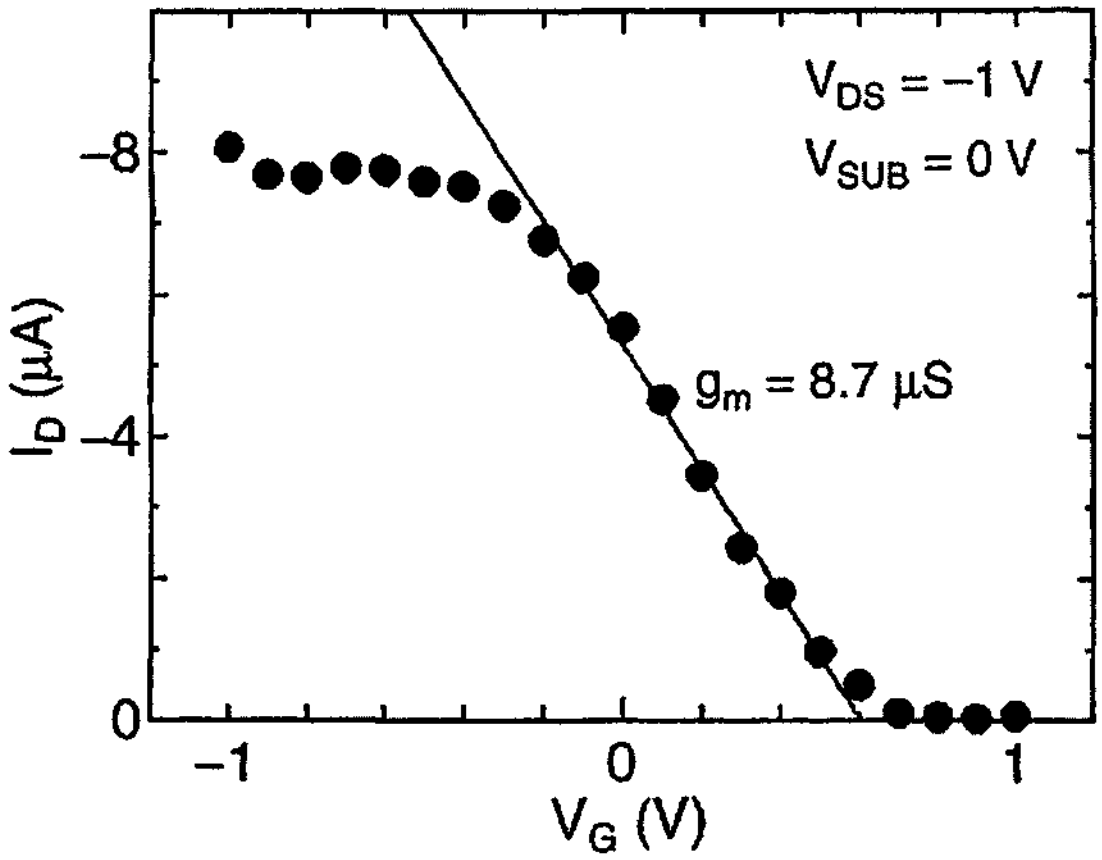

Figure 12. I_D as a function of V_G at V_{DS} = -1V.

The transconductance g_m is defined by:

$$g_m = \left| \frac{\Delta I_D}{\Delta V_G} \right|$$

and is found to be 8.7 μs for the linear range. For $V_G < -0.4V$, V_G dependence of I_D becomes smaller and saturates to $I_D = -7.5$ μA. It is plausible that parasitic resistance R_p dominates the channel resistance in the gate voltage range. Experimentally, $R_P = 130$ kΩ. Experimentally observed transconductance g_m is smaller than intrinsic transconductance g_m^i due to the existence of source resistance R_S and is given by:

$$g_m = \frac{g_m^i}{\left(1 + R_S g_m^i\right)}$$

Thus,

$$g_m^i = \frac{g_m}{\left(1 - g_m R_P / 2\right)} = 20\mu s$$

by assuming that the device is so symmetric that R_S is half of R_P. The intrinsic transconductance g_m^i is found be over twice the measured transconductance g_m. This result shows that transconductance can be improved drastically by decreasing parasitic resistance. We expect the performance of CNTFETs will advance further by improving CNT quality and optimizing device structures.

References

1. Lijima, S., Nature 354, 56 (1991).
2. Mintmire, J.W., Dunlap, B.I., white, C.T., Phys. Rev. Lett. 68, 631 (1992).
3. Hamada, N., Sawada, S., oshiyama, A., ibid., p.1579.
4. Dresselhaus, M.S., Dresselhaus, G., Eklund, P.C., Science of Fullerenes and Carbon nanotubes (Academic press, New York, 1996).
5. Chico, L., Crespi, V.H., Benedict, L.X., Lovie, S.G., Cohen, M.L., Phys. Rev. Lett. 76, 971 (1996).
6. Chico, L., Benedict, L.X., Lovie, S.G., Cohen, M.L., Phys. Rev. B54, 2600 (1996).
7. Saito, R., Dresselhaus, G., Dresselhaus, M.S., ibid. 53, 2044 (1996).
8. Charlier, J., Ebbesen, T.W., Lambin, P., ibid., p.11108.
9. Tans, S.J., Devoret, M.J., Dai, H., Thess, A., Smalley, R.E., Greetings, L.J., and Dekker, C., Nature (London) 386, 474 (1997).
10. Bockrath, M., Cobden, D.H., Mc Euen, P.L., Chopra, N.G., Zettl, A., Thess, A. and Smalley, R.E., Science 275, 1922 (1997).
11. Tans, S.J., Verschuren, A.R.M., and Dekker, C., Nature (London) 393, 49 (1998).
12. Tsukagoshi, K., Alphenaar, B.W., and Ago, H., Nature (London) 401, 572 (1999).
13. Collins, P.G., Zettl. A., Bando, H., Thess, A., and Smalley, R.E., Science 278, 100 (1997).
14. Fuhrer, M.S., Nygard, J., Shih, L., Farero, N., Yoon, Y., Mazoni, M.S.C., Choi, H.J., Ihm, J., Lovie, S.G., Zettl, A., and Mc Euen, P.L., Science 288, 494 (2000).
15. Saito, R., Dresselhaus, G., Dresselhaus, M.S., "Physical Properties of carbon Nanotubes" published by " Imperical collegc prcss" 2003.
16. Sze, S. M., Physics of Semiconductor Devices, 2nd ed. (Wiley, New York, 1981).
17. Saito, R., Fujita, M., Dresselhaus, G., and Dresselhaus, M.S., Phys. Rev. B.46, 1804 (1992).

18. Thess, A., Lee, R., Nikolaev, P., Dai, H., Petit, P., Robert, J., Xu, C., Lee, Y.H., Kim, S.G., Rinzler, A.G., Colbert, D.T., Scuseria, G.E., Tomnek, D., Fischer, J.E., Smalley, R.E., Science 273 (1996) 483.
19. Fumiyuki Nihey, Hiroo Hongo, Yukinori Ochiai, Masako Yudasaka, and Sumio Lijima, Jpn. J. Appl. Phys. Vol.42 (2003) pp. L 1288-L1291.